BNL-31486

BNL--31486

DE82 018062

CHAPTER

THE IBA IN DEFORMED NUCLEI

R. F. Casten and D. D. Warner

Brookhaven National Laboratory, Upton, New York, 11973, USA

Outline:

I. INTRODUCTION AND BACKGROUND

- A. Motivation and Basic Concepts of the IBA
- B. Some Tests of the IBA

II. IBA CALCULATIONS FOR DEFORMED NUCLEI

- A. The SU(3) Limit and Broken SU(3) Calculations
- B. IBA Calculations for ^{168}Er
- C. Other Deformed Nuclei

III. THE IBA AND GEOMETRICAL MODELS IN DEFORMED NUCLEI

- A. Bandmixing Formalism: Mikhailov Plots
  - A.1. γ-g mixing
  - A.2. β-γ mixing
- B. Origin of $\beta\rightarrow\gamma$ Transitions in the IBA
- C. Bandmixing Analysis of $\beta\rightarrow\gamma$ Transitions in ^{168}Er

IV. SIMPLE INTERPRETATION OF THE IBA IN DEFORMED NUCLEI

- A. Reduction of the Hamiltonian
- B. Transformation to SU(3) Basis
- C. Composition of Transition Rates

I. INTRODUCTION AND BACKGROUND

A. Motivation and Basic Concepts of the IBA

As Talmi (1979) and others (e.g., Bohr and Mottelson, 1975) have repeatedly emphasized, the Shell Model, though in principle the preferred description of nuclear structure, is impractical in heavy nuclei for all but those few nuclei close to major closed shells. Much of the history of nuclear structure physics, therefore, has consisted of various attempts at simplification. By definition each of these simplification schemes will produce only a small subset of the possible excitations: the hope of each is that it selects out an "important" subset, generally those which constitute low lying, collective excitations which have been found empirically to characterize the first MeV or two of excitation in the majority of nuclei. These attempts have, in the main, followed two general paths. In one, an explicitly macroscopic approach, a nuclear shape is assumed, and low lying collective excitations emerge as geometric motions (rotations and vibrations) of that shape. The model of Bohr and Mottelson (1975 and refs. therein) for deformed nuclei, with its offshoots and extensions, is the most successful of these. In the other, somewhat more microscopic, approach, one truncates the Shell Model fermion space. The IBA, particularly its neutron-proton version, called IBA-2, has come to be viewed in this light. The IBA-1 does not distinguish proton and neutron bosons and is treated phenomenologically; nevertheless to the extent to which its parameters can be obtained by projection from IBA-2, it can be thought of as effectively partaking of this same class. The s and d bosons taken as building blocks for the IBA are generally considered as comprising a boson space arising by a mapping from a mini-fermion space which incorporates only those states consisting of correlated pairs of particles coupled to spin 0 and 2. Thus the assumption is that it is only this subset of the total fermion space which is important in the description of the low lying collective degrees of freedom.

It is important to recognize the enormity of the truncation involved here so as to appreciate the a priori expected limitations of the approach and to emphasize the wonder that it works at all. Figure 1 illustrates the truncation with Talmi's example of $_{62}{}^{154}Sm_{92}$ which has a total of 22 valence neutrons and protons. From the available orbits for these fermions one can construct (Talmi, 1979) over 3×10^{14} 2^+ states. The IBA-1 is effectively then a filter which selects just 26 of

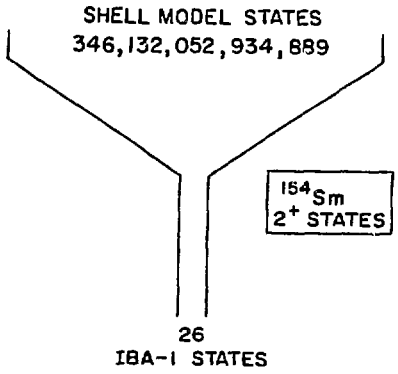

Fig. 1. Schematic illustration of the truncation included in the IBA (after Talmi, 1979).

these. The point here concerning the intractability of the Shell Model is two-fold: first, the full calculation (diagonalzation) of $3x10^{14}$ states is impossible and second, were it computationally feasible, the results would be effectively meaningless. How, for example, could the origin of regularities arising from wave functions with this many components be understood? Yet there is abundant empirical evidence that regularities and therefore simplicities do exist and therefore that this complexity may not be needed.

The formulation of the IBA has been treated many times (Arima and Iachello, 1975, 1976, 1978a, 1978b; Iachello, 1979, 1981a, 1981b; Scholten, Iachello and Arima 1978; and Scholten, 1980) and will not be repeated here except as needed for our particular discussion. The treatment below centers almost solely on the IBA-1. Although this phenomenological version of the IBA neglects a seemingly crucial distinction between proton and neutron bosons, it has been highly successful and, it turns out, particularly transparent physically. While the IBA-2 (Otsuka, Arima and Iachello, 1978; and Otsuka and co-workers, 1978) tends to look for its physical interpretation to the microscopic shell model, the IBA-1, largely because it naturally contains three limiting symmetries, which can each be associated with a well defined nuclear shape, has generally looked towards geometrical models for physical interpretation. Beyond some practical computational advantages of the IBA-1, its use should be particularly appealing for deformed nuclei which are perhaps the most well understood in the geometrical framework. Moreover, the IBA-2 tends to differ most from the IBA-1 where the proton and neutron bosons are constructed from fermions in widely different regions of their respective major shells. Such is not the case in deformed nuclei. (At the end of this paper, there will be a brief return to the relation between the IBA-2 and a modified version of the IBA-1: henceforth the notation IBA will be used to mean IBA-1 unless the context demands a specific distinction with IBA-2.)

In the IBA, one assumes that the low lying excitations can be constructed from a fixed number, N, of bosons, where N is half the number of proton particles (or holes) and neutron particles (or holes) from their respective nearest closed shells and that these bosons can occupy states with angular momentum 0 (s bosons) or 2 (d bosons). [Numerous extensions (albeit also complications) of the model to

include higher angular momentum bosons (e.g., g bosons with L=4), negative parity states (f bosons or p bosons), or to account for intruder states via s',d' bosons constructed from different subsets of shell model fermion states, have been carried out, in some cases with considerable success. Generally such extensions deal with higher lying or special states and will only be casually mentioned here. For references to such topics, see Sage and Barrett, 1980; Wu, 1982; Lin, 1982; Duval and Barrett, 1981b; Sambataro and Molnar, 1982; and Van Isacker and co-workers, 1981, 1982.]

The s and d bosons are allowed to interact via a boson Hamiltonian, expressed in a second quantized formalism (with operators s,s^+,d,d^+) including terms that change the d boson number, n_d, by up to two (while conserving $N=n_s+n_d$). For our purposes, and indeed for most IBA-1 applications, a more convenient version of the resulting Hamiltonian is expressed in terms of operators (Q, P, etc.) that can be thought of as quadrupole, pairing, etc. operators acting on the boson space. A somewhat simplified version, adequate for most of the present discussion, is

$$H = \varepsilon n_d - \kappa Q\cdot Q - \kappa' L\cdot L + \kappa'' P\cdot P + \ldots\ldots \qquad (1)$$

where ε is the d boson energy,

$$Q \propto (s^+\tilde{d}+d^+s)^{(2)} + \frac{\chi_Q}{\sqrt{5}}(d^+\tilde{d})^{(2)}$$

$$P \propto (d^+d^+ss)^{(0)} + \chi_p(s^+s^+\tilde{d}\tilde{d})^{(0)} \qquad (2)$$

$$L \propto (d^+\tilde{d})^{(1)}$$

More precise definitions and discussion of these operators, including numerical constants, are given in Iachello (1981a, 1981b). In Eq. 1, L is a diagonal boson angular momentum operator that conserves d boson number, and the neglected terms in Eq. 1 are also d-boson number conserving terms that may be used to fine tune energy or transition rate calculations. (One of these, a term $T_3(d^+d^+)^{(3)}(\tilde{d}\tilde{d})^{(3)}$, is crucial to the O(6) limit and will be returned to in Section V). Note that the term in Q·Q has $\Delta n_d=0,1,2$ components while that in P·P has $\Delta n_d=0,2$ components. The internal constant χ_Q in Q is usually chosen so that Q becomes a generator of SU(3), that is, $\chi_Q = -\sqrt{35}/2 \approx -2.958$. (See last chapter for a re-formulation incorporating a variable χ_Q.)

The elegance of the Hamiltonian of Eq. 1 is manifest when the group structure of the IBA is considered. Since the components of the s and d bosons span a 6 dimensional space, the IBA-1 can be expressed in terms of the group U(6) and its subgroups. A group decomposition shows (Iachello, 1979, 1981a) that there are three distinct chains, each corresponding to a particular nuclear symmetry, namely SU(5), an anharmonic vibrator, SU(3), a special case of the deformed rotor, and O(6), a γ-unstable vibrator. For each of these three limits the characteristic wave functions are generated by specific terms in Eq. 1: SU(5) by the εn_d term, SU(3) by the $\kappa Q\cdot Q$ term and O(6) by the $\kappa''P\cdot P$ term. These terms are those that separate families of levels in each limit according to major quantum numbers: n_d for SU(5), (λ,μ) for SU(3), and σ for O(6). In all three limits the diagonal $\kappa' L\cdot L$ term may also be added to separate states of different spin but otherwise identical quantum numbers. In O(6), the T_3 term mentioned above is also used to separate states according to another quantum number τ. The low lying levels of each symmetry are shown in Fig. 2.

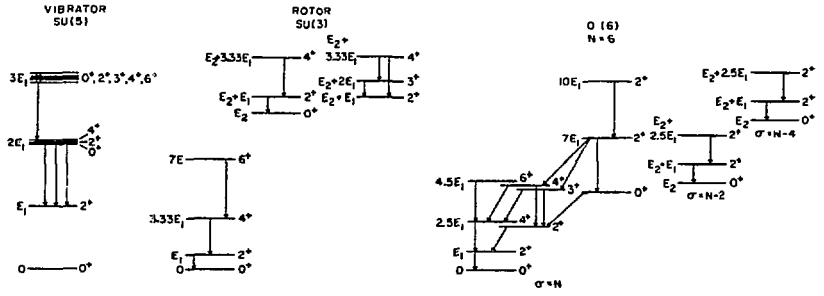

Fig. 2. Some low lying levels and E2 transitions in each limit of the IBA. (To avoid cluttering, the $\beta' \to \gamma'$ transitions, though characteristic of SU(3), are not shown.)

Important characteristics of each limit are the E2 transition rates. Each limit carries with it certain specific selection rules as well as simple analytic expressions for the relative sizes of allowed transitions. To define the E2 properties of each limit, or, indeed, of any IBA calculation, one needs to specify the E2 operator, T(E2). It is given by

$$T(E2) = \alpha[(s^{+}\tilde{d}+d^{+}s)^{(2)} + \frac{\chi}{\sqrt{5}}(d^{+}\tilde{d})^{(2)}] \qquad (3)$$

where α is an overall normalization constant. If one demands that, in the limiting symmetries, the operator be composed of generators of the group then χ=0 for O(6) and -2.958 for SU(3). In intermediate situations χ is usually treated as a free parameter, allowed to vary from 0 to -2.958. Some of the principal transitions for each limit are included in Fig. 2.

It is convenient and useful to illustrate some of the preceeding ideas by the symmetry triangle shown in Fig. 3. The triangle highlights an extremely important point. While one may insert any combination of parameters into Eq. 1, nuclear transitions from one symmetry scheme to another proceed most directly along one of the legs. A first order approach to the calculation of such transition regions then corresponds simply to a one-parameter progression along the leg. The one parameter is the ratio of the coefficients of the terms controlling each vertex. These characteristic transition parameters are indicated in the figure along with specific nuclei that seem to reflect these transitional progressions. Of course, while fine tuning of any actual calculation may involve other terms in Eq. 1 (including the terms not shown), it has been found so far that the simpler treatment just introduced accounts for all the broad features and many of the fine details as well. Except for occasional caveats below, the discussion here will be couched in terms of the simpler scheme.

The wave functions in the IBA are normally expressed in terms of the basis states of the SU(5) limit, which are determined by four quantum numbers n_d, n_β, n_Δ and the spin L, where $n_\beta(n_\Delta)$ is the number of pairs (triplets) of bosons coupled to spin zero. The lowest states of the SU(5) symmetry and their quantum numbers are illustrated in more detail in Fig. 4. These will, of course, be instantly familiar to the reader as analagous to the eigenstates of the harmonic vibrator.

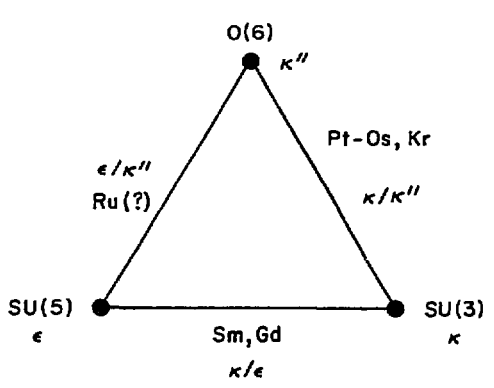

Fig. 3. A schematic description of symmetries (vertices) and transition regions (legs) in the IBA. Alongside each symmetry vertex the coefficient of the characteristic term in Eq. 1 is given.

As noted, the terms in P•P and Q•Q in Eq. 1 do not conserve n_d and thus mix the basis states. The wave functions for the lowest three 0^+ states of the three limits are given, for N=6, in Table 1. For O(6) the only non-diagonal term is P•P and thus the wave functions, though clearly more complicated than in SU(5), display evident regularities. Only basis states differing by a zero coupled pair of d bosons (i.e., by $(\Delta n_d, \Delta n_\beta, \Delta n_\Delta) = (2,1,0)$) are present in a given O(6) state. The τ quantum number (Arima and Iachello, 1978b) distinguishing states within a given major σ family in this limit is directly related to the lowest n_d value occuring in each wave function (e.g., the ground state and 0^+_2 state have $\tau=0$, the 0^+_3 level has $\tau=3$). The SU(3) limit is generated by the Q•Q term which, having $\Delta n_d=0,1,2$ terms, more thoroughly mixes all the SU(5) basis states and it

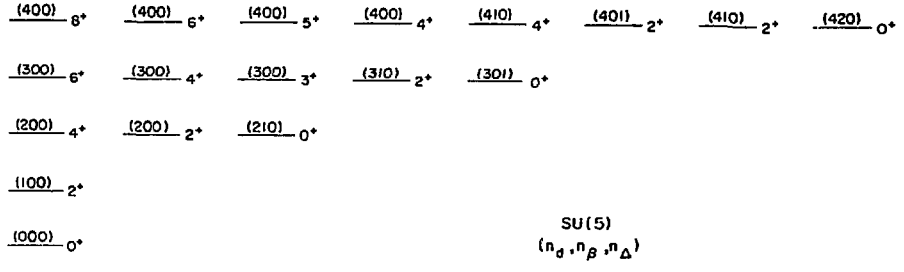

Fig. 4. States of the SU(5) limit with $n_d \leq 4$. These are the usual basis states of the IBA and, in particular, of the IBA-1 code PHINT (Scholten, 1977).

TABLE 1 Wave functions expressed in the SU(5) basis for the first three 0^+ states in each limit of the IBA

		Basis States $(n_d n_\beta n_\Delta)$						
State [a]	Limit	(000)	(210)	(301)	(420)	(511)	(602)	(630)
0^+_1	SU(5)	1	0	0	0	0	0	0
	O(6)	-.43	-.75	0	-.491	0	0	-.095
	SU(3)	.134	.463	-.404	.606	-.422	-.078	.233
0^+_2	SU(5)	0	1	0	0	0	0	0
	O(6)	.685	.079	0	-.673	0	0	-.269
	SU(3)	.385	.600	-.204	-.175	.456	.146	-.437
0^+_3	SU(5)	0	0	1	0	0	0	0
	O(6)	0	0	-.866	0	-.463	0	0
	SU(3)	-.524	-.181	-.554	.030	-.114	-.068	-.606

a) The states are ordered for pedagogical clarity and not necessarily in the order of increasing energy: indeed, the $\tau=3$ 0^+ state in O(6) (here labelled 0^+_3) is usually the 0^+_2 state (see Fig. 2, for example).

is clear from Table 1 that the SU(3) wave functions are rather complex. Such complexity will also characterize the wave functions from realistic calculations for deformed nuclei which (see below) are usually carried out by introducing some degree of symmetry breaking to the SU(3) limit. It is already evident, then, that it will be difficult to gain an easy physical feeling for the structure of such wave functions from their SU(5) decomposition. This point will be returned to later.

B. Some Tests of the IBA

It is not the purpose here to survey the empirical tests of the IBA. This has been done recently (Casten, 1980, 1981). However, to place the following discussion in context and to provide some suggested background reading material, it is worthwhile to mention a few selected studies. One of the first successes of the IBA was its prediction of the O(6) symmetry (Arima and Iachello, 1978b). This was accompanied almost simultaneously by its empirical observation in ^{196}Pt (Cizewski et al., 1978). One of the principal attractions of a symmetry scheme is that it provides a new benchmark for the interpretation of nuclei that deviate from it. Thus, for example, level energy sequences close to an I(I+1) dependence are unintelligible without a foreknowledge of the rotor symmetry: with it, they simply

reveal a rotational nucleus with small interactions (e.g., rotation-vibration coupling) breaking the symmetry. Similarly, the Pt-Os nuclei have always been considered extraordinarily complex, reflecting the coupling and interactions of prolate, oblate, hexadecapole and axially asymmetric degrees of freedom. However, with the manifestation of the O(6) limit in ^{196}Pt, it became immediately obvious to treat this region as initiating an O(6) → SU(3) transition down the right leg of the symmetry triangle (Casten and Cizewski, 1978; for related IBA-2 calculations see Duval and Barrett, 1981a; and Bijker and co-workers, 1980). The Kr isotopes also reflect the same transition leg (Kaup and Gelberg, 1979). Completely analogously, but more familiar because of similar, prior geometrical model interpretations, is the treatment of the Sm isotopes in terms of a vibrator to rotor, or SU(5) → SU(3) transition (Scholten, Iachello and Arima, 1978), corresponding to the base of the symmetry triangle. Very recently Stachel, Van Isacker and Heyde (1982) have suggested that the left leg (SU(5) toward O(6)) is at least partially reflected in the Ru isotopes although, here, the correspondence is less clear cut.

Conspicuously absent in the above listing is a detailed treatment of a well deformed nucleus. However, this is a crucial test for several reasons. First, such nuclei represent the largest single class of nuclei. Secondly, critiques of the IBA have suggested (Bohr and Mottelson, 1980) that it is in exactly such nuclei that any shortcomings should be most evident. Finally, the IBA in deformed nuclei inherently contains some characteristic predictions that contrast sharply with those of the usual geometrical model interpretation and which therefore merit extensive testing.

However, precisely because these differences center on hard-to-observe low energy transitions between bands at 1-2 MeV, the requisite empirical information has not been available until a recent (n,γ) study of ^{168}Er by Davidson and co-workers (1981). The result of that study is a complete set of about 20 rotational bands up to 2 MeV and a very thorough set of transitions connecting these states. Since the full set of K=0 and 2 bands below 2 MeV was disclosed, a detailed test of the IBA became possible, including whether or not there is a one-to-one correspondence between the empirical and model states.

The rest of this paper is devoted to a description of the application of the IBA to deformed nuclei, with special emphasis in the next section on the basic characteristics of the IBA predictions for such nuclei and a comparison with the ^{168}Er level scheme. Following this will be a discussion of the IBA predictions in terms of geometrical concepts and then a particularly simple interpretation of the calculations for deformed nuclei in terms of a re-expansion of IBA wave functions and transition rates and a transformation of the Hamiltonian into the SU(3) basis. Lastly, a recently proposed modification to the formulation of the IBA-1 will be discussed which relaxes the assumption that the quadrupole operator of the Hamiltonian should take the form of the SU(3) generator.

II. IBA CALCULATIONS FOR DEFORMED NUCLEI

A. The SU(3) Limit and Broken SU(3) Calculations

The starting point for any IBA calculation of deformed nuclei is the SU(3) limit (Arima and Iachello, 1978a), illustrated in more detail for N=16 in Fig. 5 and generated by any combination of the Q•Q and L•L terms in Eq. 1. The levels are grouped into representations defined by the quantum numbers (λ,μ). Within each representation appear one or more level sequences that resemble rotational bands. The eigenvalue expression is:

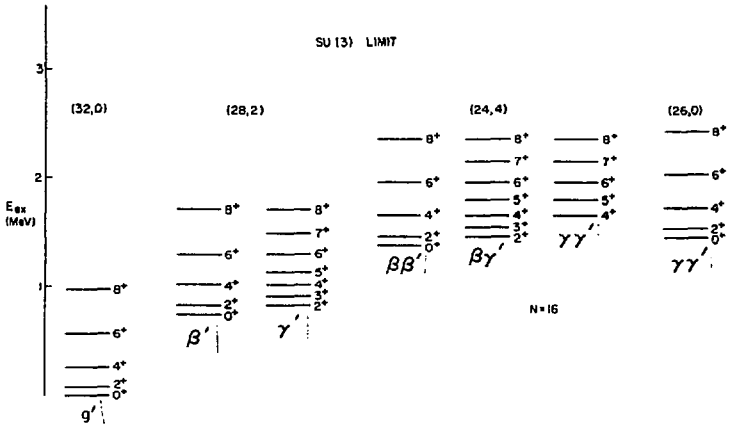

Fig. 5. The lowest four representations of the SU(3) limit showing the level groupings into rotational bands. The labels g', β', γ', etc. are a shorthand nomenclature for these bands which reflects their approximate similarity to the corresponding geometrical excitations but which also, by virtue of the primes, emphasizes their distinctiveness.

$$E(\lambda,\mu,L) = (3/4\kappa - \kappa')\, L(L+1) - \kappa C(\lambda,\mu)$$
$$\text{where } C(\lambda,\mu) = \lambda^2 + \mu^2 + \lambda\mu + 3(\lambda+\mu) \qquad (4)$$

The coefficients κ and κ' are those of Eq. 1. Only the Q•Q term determines the overall energy scale of the different representations. It is immediately clear that the SU(3) limit closely resembles a deformed rotor. There is a ground state rotational band followed, at higher energy, by two bands which seem to resemble the familiar β (K=0) and γ (K=2) bands of the Bohr-Mottelson picture followed by still higher lying bands which mirror the K=0 ββ (double β), the K=2 βγ and the K=0 and 4 γγ (double γ) vibrations. [In principle, since the states of a given spin within a representation are degenerate in SU(3), the separation into distinct bands effectively implies a specific choice of axes, that is, a projection onto states of good (or nearly good) K value. In practical calculations, such a projection can be introduced by an infinitesimal perturbation of the pure SU(3) Hamiltonian, for example, by a minute ϵn_d term in Eq. 1.]

Despite these similarities to the geometrical model it is already evident from Fig. 5 that the SU(3) limit must be a special case of a deformed rotor because of the band degeneracies. In most empirical deformed nuclei the β and γ bands are not degenerate and thus, to calculate such cases, one is forced to break the SU(3) symmetry.

It is well to emphasize at this point that, in the following, the phrase "geometrical model" will refer to the simplest harmonic version of the model. This geometric model is an extreme simplification and cannot fairly be expected to apply to real nuclei without the introduction of further interactions and

perturbations. Comparisons below between the IBA and this model are therefore not generally intended to be pejorative to it but rather, by comparison with it, to elucidate characteristic features of the IBA and to better understand the structure of the IBA in deformed nuclei by reference to familiar geometric concepts. To highlight both the similarities and differences between the geometrical model and the SU(3) limit of the IBA, it is best to introduce a somewhat tedious but necessary notation: the the IBA SU(3) intrinsic excitations will be denoted by a primed geometrical terminology g', β', γ', ββ', βγ', γγ' while related excitations in a broken SU(3) calculation, or the empirical excitations themselves, will generally be referred to within quotation marks (e.g., "β", "γ", etc.).

As just noted, the "β" and "γ" bands in actual nuclei are seldom degenerate. In particular, in the majority of well deformed nuclei, the "β" band is above the "γ" band. This feature can be obtained from the Hamiltonian of Eq. 1 in a simple way. As shown in Fig. 2, the O(6) limit, which is generated by the P•P term in Eq. 1, is characterized by a low lying level sequence built on the 2^+_2 level that is reminiscent of a "quasi γ" band and with the lowest 0^+ excitation considerably higher. Thus one might suspect that the use of a small P•P term to break the SU(3) symmetry might be effective in raising the "β" band energy. This is indeed correct and it appears that, aside from possible fine tuning, it is possible to represent deformed nuclei with $E_{"\beta"} > E_{"\gamma"}$ by the Hamiltonian

$$H = -\kappa Q\cdot Q - \kappa' L\cdot L + \kappa'' P\cdot P \qquad (5)$$

In this scheme, the P•P perturbation has little effect on the ground and "γ" band energies. Thus, the parameters κ and κ' are still fixed by using the SU(3) eigenvalue expression, Eq. 4, for the first two 2^+ states. Then, the one remaining parameter, κ", is varied to fit the energy of the first K=0 excitation.

Among the most important signatures of nuclear structure are nuclear transition rates. In deformed nuclei, the most crucial of these involve E2 transitions, which will be discussed throughout this paper. However, it should be noted that M1 transitions can also be described in the IBA framework. They will not be discussed here, and the reader is referred to Warner (1981) for a discussion of this subject.

The E2 selection rules for SU(3) are $\Delta(\lambda,\mu)=0$, that is, only transitions within a representation are allowed. The limit is characterized by strong intraband transitions, weaker ones between bands belonging to the same representation and no transitions between bands of different representations. Although the strong intraband transitions are a familiar feature of the geometrical deformed rotor, the other features lead to results that are distinctly different from the geometrical model of harmonic β and γ vibrations in which, since E2 transitions may change the β or γ phonon number by one, β→g and γ→g transitions are allowed but β→γ transitions are forbidden. In the SU(3) limit of the IBA, the latter transitions are allowed while those to the ground band are forbidden. Thus the starting point of the geometric model and the SU(3) limit are superficially similar but substantially different in detail. Figure 6 summarizes the key differences for the lowest bands in the two models, each in its extreme or purest form: the SU(3) limit for the IBA and pure β, γ vibrations for the geometric model. The dashed lines represent decay modes that are strictly forbidden but which may be introduced by perturbations in the respective schemes.

Many features of the application of the IBA in deformed nuclei, and of its relationship to the geometrical picture, can be understood by a study of the role of the E2 operator in the SU(3) limit of the model. This subject is dealt with in detail in Warner and Casten (1982b). Some of the essential results are summarized

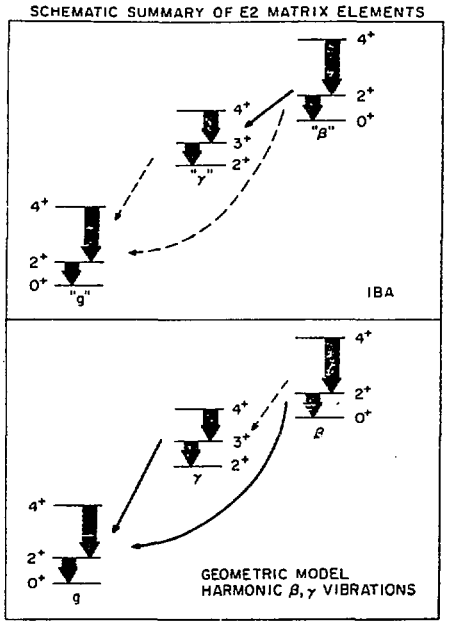

Fig. 6. Comparison of the allowed and forbidden transitions involving the lowest bands in the SU(3) limit of the IBA and in the geometrical model. For simplicity in the former, the β' and γ' bands are displaced in energy to resemble typical deformed nuclei; the transitions are those of the SU(3) limit.

here. As long as $\Delta(\lambda,\mu) \leq 4$ each of the operators $(s^{+}\tilde{d}+d^{+}s)$ and $(1/\sqrt{5})(d^{+}\tilde{d})$ in T(E2) (see Eq. 3) gives a finite contribution to an inter-representation matrix element. The fact that the total inter-representation matrix element is zero in the SU(3) limit results because these contributions are always in the precise ratio of 2.958:1. Thus, when $\chi = -2.958$, the two terms cancel. Hence, the use of a χ value different from -2.958 will lead to finite inter-representation transitions even though the wave functions remain pure SU(3) in structure.

The constancy in the relative matrix elements of the two operators in T(E2) leads to an interesting and useful result. Denoting the matrix elements of $(s^{+}\tilde{d}+d^{+}s)^{(2)}$ and $(1/\sqrt{5})(d^{+}\tilde{d})^{(2)}$ by T_1 and T_2, respectively, one has, for any inter-representation transition with $\Delta(\lambda,\mu) \leq 4$, $\langle i \| T(E2) \| f \rangle = T_1 + \chi T_2$. But, as noted above, $T_2 = (1/2.958)\, T_1$. Thus the matrix element can be rewritten $\langle i \| T(E2) \| f \rangle = T_1\,(1 + \chi/2.958)$. Then any ratio of inter-representation matrix elements becomes

$$\frac{\langle i \| T(E2) \| f \rangle}{\langle i' \| T(E2) \| f' \rangle} = \frac{T_1}{T_1'} \frac{(1 + \chi/2.958)}{(1 + \chi/2.958)} = \frac{T_1}{T_1'} \qquad (6)$$

independent of χ.

This, in turn, leads to a particularly simple interpretation of the "multi-phonon" excitations of the SU(3) limit via a comparison of their predicted relative E2 decay modes with those expected from harmonic β and γ vibrations. The result is that the behavior of those double excitations with K=2 and K=4 closely follows that of the corresponding multiple geometrical excitations ($\beta\gamma$ and $\gamma\gamma$), but that for the "multiple" modes with K=0, of which there are two, the decays differ from expectations arising in a phonon picture. It is, however, possible to recover a simple interpretation if it is assumed that each of these K=0 bands is a linear combination of the pure double modes. Then one can solve for the coefficients of these amplitudes by using the transition strengths for the pure geometrical double vibrations and by reproducing the calculated SU(3) B(E2) values with the composite wave functions. The results depend slightly on which band members are chosen but to a close approximation one can write

$$\Psi_{K=0}(2N-8,4) \approx \sqrt{0.67}\ \beta\beta' + \sqrt{0.33}\ \gamma\gamma'$$

$$\Psi_{K=0}(2N-6,0) \approx +\sqrt{0.33}\ \beta\beta' - \sqrt{0.67}\ \gamma\gamma'$$

(The choice of phase convention is arbitrary.) Thus the labels $\beta\beta'$ and $\gamma\gamma'$ in Fig. 6 and in all subsequent discussions are a shorthand notation that identifies only the dominant amplitudes in the K=0 bands of the (2N-8,4) and (2N-6,0) representations, respectively. This simplification should be borne in mind when the terminology is used below.

As noted above, inter-representation transitions will occur even in the SU(3) limit if $\chi \neq -2.958$. It is thus worthwhile discussing the behavior of such transitions as a function of χ and this is illustrated on the left in Fig. 7. The $\beta'\rightarrow g'$ and $\gamma'\rightarrow g'$ transitions go to zero for $\chi = -2.958$ whereas the intense intra-band intra-representation $2^+_{g'}\rightarrow 0^+_{g'}$ transition is insensitive to χ and so is the inter-band intra-representation $2^+_{\gamma'}\rightarrow 0^+_{\beta'}$ transition. Note, moreover, that the $\gamma'\rightarrow g'$ B(E2) value is always larger than the $\beta'\rightarrow g'$ value and, of course, from our previous argument (Eq. 6), by a constant factor.

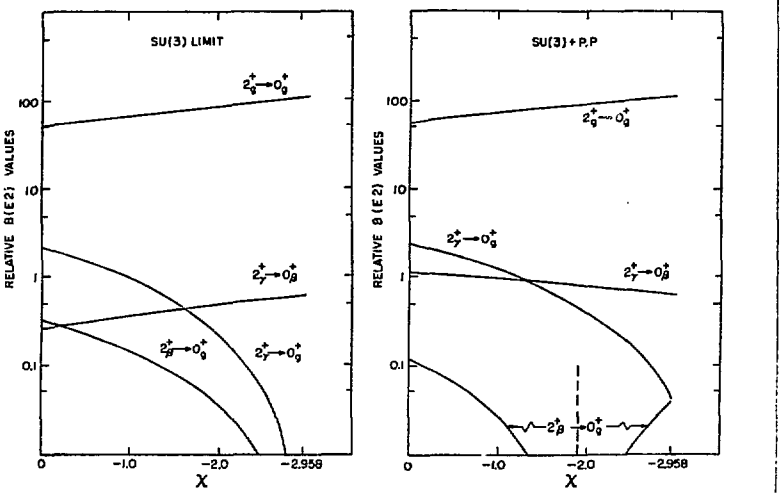

Fig. 7. Dependence of several transitions on the parameter χ of the E2 transition operator. Left: SU(3) wave functions. Right: A broken SU(3) calculation. (From Warner and Casten, 1982b).

These general characteristics are preserved in the broken SU(3) limit as shown on the right in Fig. 7 for a typical value of κ''. The intra-representation transitions are hardly affected by the perturbation. The "γ"→"g" transitions exhibit approximately the same behavior as in SU(3) except that they no longer vanish for $\chi = -2.958$. The most important change is that the "β"→"g" transitions now vanish for a different value of χ (≈ -1.9). Once again, they are always smaller than the "γ"→"g" transitions. To reiterate, for broad ranges of the parameters, both of the Hamiltonian and the E2 operator, ranges which encompass most deformed nuclei, the IBA clearly and unequivocably predicts that a) "β"→"g" transitions are weaker than "γ"→"g" transitions and b) "β"→"γ" transitions are stronger than "β"→"g" transitions.

It is well known empirically that the "γ"→"g" transitions in deformed nuclei are collective. Perhaps not as well recognized is the fact that the B(E2) ratio $B(E2{:}2^+_\gamma \rightarrow 0^+_g)/B(E2{:}2^+_g \rightarrow 0^+_g)$ falls in a rather narrow range centering on ≈ 0.03. These systematics, as well as those for the "β" band (discussed below) are collected for the rare earth region in Fig. 8. The sensitivity of the B(E2) ratio $B(E2{:}2^+_\gamma \rightarrow 0^+_g)/B(E2{:}2^+_g \rightarrow 0^+_g)$ to χ and its relative insensitivity to κ'', make this empirical quantity particularly useful for fixing the value of χ. Then the narrow empirical spread of this ratio leads to a correspondingly narrow range of possible χ values, namely, $-1.2 \leq \chi \leq -0.5$, which is then applicable to all deformed nuclei (with $E"\beta" > E"\gamma"$). (See Warner and Casten, 1982; and McGowan, 1981.)

An important consequence arises from this narrow range of permitted χ values in that many aspects of IBA calculations for deformed nuclei may be approximately calculated by taking a "global" mean value of $\chi = -0.85$. This allows a rather general study of the structure of IBA predictions for deformed nuclei that does not depend on the details of a given nucleus.

B. IBA Calculations for ^{168}Er

As noted in the Introduction, the empirical level scheme for ^{168}Er is an ideal test case for the IBA in deformed nuclei. It is centrally located in the rare earth region, is well deformed, exhibits sufficiently low lying intrinsic K=0 and 2 excitations (β and γ bands in geometric terminology) that it may be possible to observe multi-phonon modes, and, now, has been thoroughly studied by a combination of (n,γ) techniques (Davidson and co-workers, 1981). The wealth of intra- and interband transitions that are essential to grouping the levels into the 20 rotational bands identified are exemplified by those shown for the lowest bands in Fig. 9. Note in particular the low energy transitions within each band and especially those between "β" and "γ" bands. These latter, "β"→"γ", transitions have seldom been observed before, and never in such detail, because, though they will be seen to represent large collective matrix elements, their empirical intensities are extremely weak due to the E^5_γ factor connecting B(E2) values and transition rates. When this is factored out, it turns out that the "β"→"γ" transitions dominate the "β"→"g" ones.

These empirical results have been subjected to a rather extensive comparison with IBA calculations in Warner, Casten and Davidson (1980, 1981). Since the "β" band empirically occurs well above the "γ" band, the scheme for broken SU(3) calculations described above (i.e., Eq. 5) was used. To reiterate, the quantities κ and κ' were obtained from the SU(3) expressions and the one parameter κ'' was varied to obtain the overall energy fit with emphasis on the 0^+_2 band. For the E2 operator, χ was adjusted to fit a single B(E2) ratio. Before examining the results it is

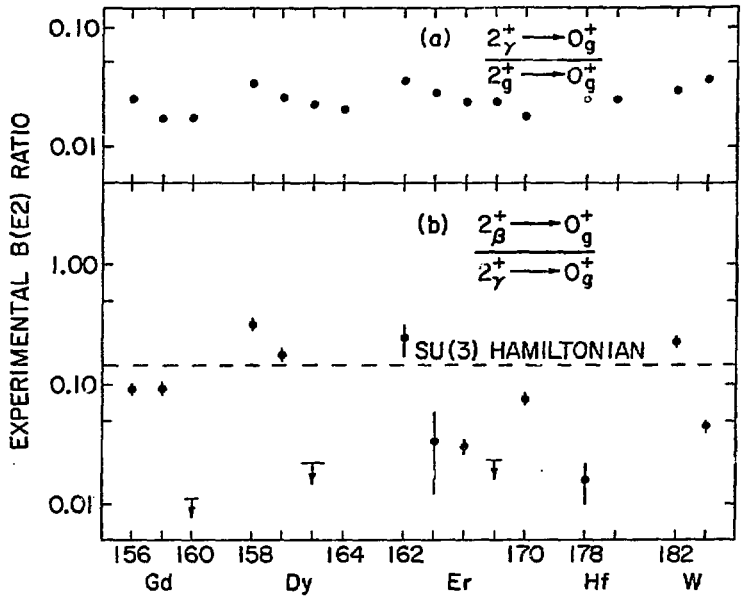

Fig. 8. Empirical systematics of B(E2) ratios from the "γ" and "β" bands of deformed nuclei (limited to those nuclei for which E"β" > E"γ"; see text). The dashed line in the lower plot is the IBA prediction (see Fig. 7) for the SU(3) limit. IBA calculations for broken SU(3) would be lower. (From Warner and Casten, 1982b.)

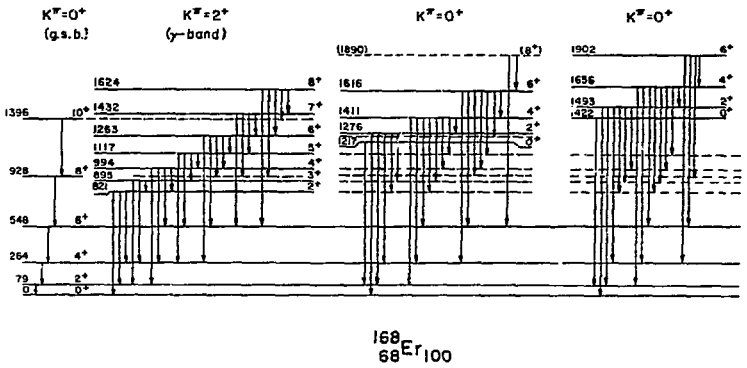

Fig. 9. Gamma-ray transitions involving the lowest bands in ^{168}Er (Davidson and co-workers, 1981).

well to strongly emphasize the specific philosophy behind these calculations. They were designed to test whether or not the IBA, treated in the simplest possible manner, appeared to be a suitable vehicle for understanding deformed nuclei. The calculations were extremely schematized and at no point was there any attempt to fine tune the calculations either by further optimization of these parameters or by the introduction of other terms into the Hamiltonian.

The results of the calculations for energy levels are shown in Fig. 10, taken from the above reference, in comparison with the empirical results. In addition to the empirical levels shown in Fig. 10 there is a $K=3^+$ band at 1653 keV. Since such a band cannot arise in an s, d boson IBA-1 framework, or indeed in the geometrical description, it is outside the scope of the present discussion and is omitted: presumably it arises either from quasi-particle excitations or, more likely, from a type of hexadecapole mode that would also appear in the IBA if a g boson were incorporated. Also omitted in Fig. 10 is a calculated K=4 band near the 0^+_3 band. Since the location of this K=4 mode has subsequently (Bohr and Mottelson, 1982) taken on some importance in critiques of these calculations we point out that the lowest empirical collective K=4 band is substantially higher, at least as high as 2055 keV (Davidson and co-workers, 1981).

Given these caveats, it is immediately evident in Fig. 10 that there exists a remarkable agreement between theory and experiment. Indeed, there is a one-to-one

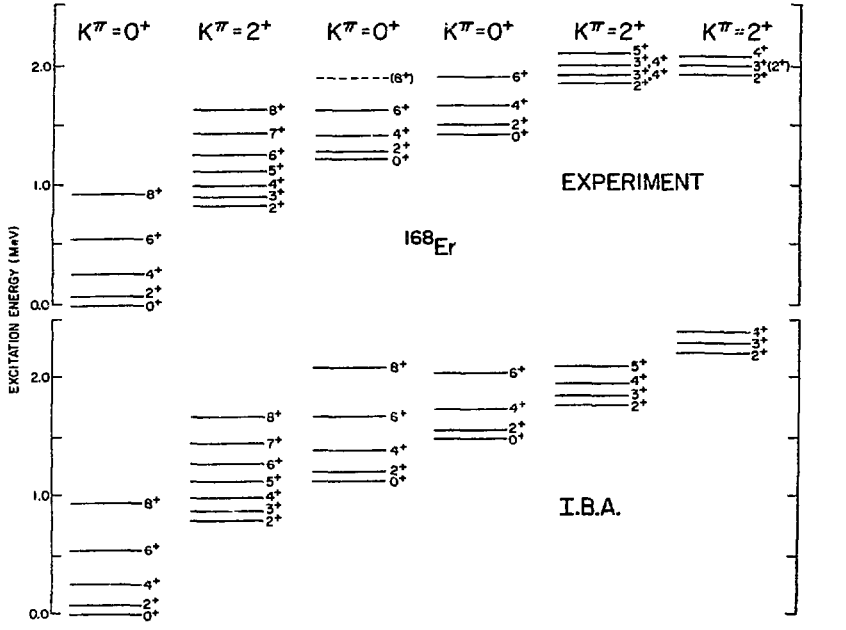

Fig. 10. Comparison of calculated and empirical levels for K=0 and 2 bands in ^{168}Er (Warner, Casten and Davidson, 1980, 1981). The IBA calculations also predict a K=4 band near the 0^+_3 band. The lowest empirical K=4 band is just above 2 MeV.

TABLE 2 Comparison of experimental and theoretical relative B(E2) values from states of the "γ" band in ^{168}Er (from Warner, Casten and Davidson, 1981)

I_i^π	I_f^π,K	Relative B(E2:$I_i \rightarrow I_f$) IBA	Exp.
2^+	0^+,0	66.0	54.0
	2^+,0	100.0	100.0
	4^+,0	6.0	6.8
3^+	2^+,0	2.7	2.6
	4^+,0	1.3	1.7
	2^+,2	100.0	100.0
4^+	2^+,0	2.5	1.6
	4^+,0	8.3	8.1
	6^+,0	1.0	1.1
	2^+,2	100.0	100.0
5^+	4^+,0	4.3	2.9
	6^+,0	3.1	3.6
	3^+,2	100.0	100.0
	4^+,2	98.5	122.0
6^+	4^+,0	0.97	0.44
	6^+,0	4.3	3.8
	8^+,0	0.73	1.4
	4^+,2	100.0	100.0
	5^+,2	59.0	69.0
7^+	6^+,0	2.7	0.74
	5^+,2	100.0	100.0
	6^+,2	39.0	59.0

correspondence between empirical and calculated states for all K=0 and 2 bands. This is particularly noteworthy when it is recalled that one has not inserted an a priori band structure into the Hamiltonian of Eq. 1. The band structure arises naturally when the Q•Q term dominates and is able to accurately mirror empirical level sequences for deformed nuclei.

Of course, the remarkable agreement in Fig. 10 must be assessed carefully. Although there is an apparent agreement in level sequences, a full test must verify that this is not fortuitous, that is, that the structure of the calculated and experimental levels is similar. This can best be done by a detailed examination of the E2 transition rates. For this comparison we take $\chi = -0.68$, the specific value fitted for this nucleus although results for the "average" value discussed earlier would not differ significantly. This comparison is presented in Tables 2 and 3. [See Warner, Casten and Davidson (1981) for further details.]

These tables show the E2 deexcitation transitions from the "γ" and "β" bands. There are a number of notable points. First, for the "γ" band, it is clear that,

TABLE 3 Comparison of experimental and theoretical relative B(E2) values from states of the "β" band in ^{168}Er (from Warner, Casten and Davidson, 1981).

I_i^π	I_f^π, K_f a)	Relative B(E2;$I_i \to I_f$) IBA	Exp.
0^+	$2^+,0$	5.5	5.5
	$2^+,2$	100.0	<28.0
2^+ b)	$0^+,0$	0.10	0.23
	$4^+,0$	0.32	1.4
	$2^+,2$	2.6	4.0
	$3^+,2$	4.9	≡4.9
	$0^+,0'$	100.0	
4^+	$2^+,0$	0.09	0.02
	$6^+,0$	0.23	0.11
	$2^+,2$	0.04	0.03
	$3^+,2$	0.63	0.35
	$4^+,2$	2.2	0.52
	$5^+,2$	2.8	0.19
	$2^+,0'$	100.0	100.0
6^+	$4^+,0$	0.07	0.02
	$8^+,0$	0.21	0.07
	$4^+,2$	0.09	0.11
	$5^+,2$	0.73	0.32
	$6^+,2$	2.0	0.93
	$4^+,0'$	100.0	100.0

a) The notation 0' refers to the 0^+_2 or "β" band (i.e., an intraband transition).

b) No multipolarity determinations could be made for the $2^+ \to 2^+_\gamma$ and $2^+ \to 3^+_\gamma$ transitions, which have, therefore, been assumed to be pure E2 in this comparison. No meaningful limit could be obtained for the $2^+ \to 0^{+\prime}$ intraband transition, and hence, the $2^+ \to 3^+_\gamma$ has been used for normalization in this case.

overall, the detailed agreement is remarkable. Not only are the relative sizes of intra- and interband transitions given correctly but the variations in detailed individual B(E2) values are excellently reproduced. Secondly, careful inspection reveals some disagreements, particularly for the higher spin states. For transitions from the 6^+ and 7^+ states these amount to factors of 2-3. These discrepancies themselves provide a significant clue to their origin since, where they exist in interband transitions, $\Delta I = +1,+2$ transitions (e.g., $6^+ \to 8^+$) are consistently under-predicted and $\Delta I = -1,-2$ transitions (e.g., $6^+ \to 4^+$) are consistently over-predicted. Moreover, the discrepancies consistently grow with increasing initial spin. These observations suggest a neglected interaction having a characteristic spin dependence and will be treated in terms of a bandmixing formalism in the next section.

For the "β" band, the detailed results in Table 3 again exhibit the excellent overall reproduction of the relative sizes of intraband, "β"→"γ", and "β"→"g" transitions which appear, both in the data and the IBA, in that order of decreasing strength. Further inspection of Table 3 shows that the detailed agreement does not approach that for the "γ" band. Both the "β"→"γ" and "β"→"g" transitions are empirically found to be on the average about a factor of 3-4 weaker than the calculated ones and there is substantial variation in the agreement for different transitions. Nevertheless, in general there is a high correlation with experiment. For example, with the exception of the $4^+_{"g"} \rightarrow 5^+_{"\gamma"}$ transition, the relative strength ordering of the transitions to a given final band is correctly given. Once again, the size and direction of the discrepancies is an important clue to an understanding of their origin. When the overall scale discrepancies of the "β"→"γ" and "β"→"g" strengths are removed, it is seen that the ΔI = 0,+1 "β"→"γ" transitions are more overpredicted than the spin decreasing transitions. This is opposite to the trend of the comparison for the "γ" band and, again, will find a ready and interesting interpretation below in terms of bandmixing.

Finally, concerning the "β" band, a comparison of the absolute transition rates (see Warner, Casten and Davidson, 1981) discloses an important point, namely that the calculated "β"→"γ" B(E2) values are about half as large as those for the "γ"→"g" transitions and thus represent a definite collective enhancement. Moreover, the empirical "β"→"g" transitions themselves are on the order of ≈0.1 s.p.u. which, though relatively small, is nevertheless larger than can be obtained for the deexcitation of any K=0 two quasiparticle excitation in this mass region, by a factor of 10^2-10^3.

While most of the emphasis here is properly placed on the key low lying collective "β" and "γ" excitations where the most complete empirical information exists, it is worthwhile commenting briefly on the higher ones (see Warner, Casten and Davidson, 1981, for details). For the 0^+_3 band, the overall agreement between experiment and theory is again qualitatively correct. The strongest interband transitions are to the "γ" band. As with the "β"→"γ" transitions their absolute intensities (empirically known only for the 4^+ initial state) appear to be somewhat overpredicted. Both theory and experiment show the transitions to the ground band to be weaker than those to the "γ" band but here there is a substantial discrepancy. The calculated values are much too small. However, in this case, the calculations are probably meaningless since the predicted B(E2) values have strengths $\approx 10^{-2}$-10^{-3} s.p.u. and therefore cannot be considered immune to small perturbations to this collective description.

To summarize the comparison between the IBA and the empirical results for ^{168}Er the following points are significant:

1. With an extremely simplified treatment, the IBA predicts a sequence of states belonging to K=0 and K=2 bands that is, on energy grounds, in a one-to-one correspondence with the known-to-be-complete set of empirical levels and bands.

2. Given the same simplified framework, the overall prediction of B(E2) values is also excellent. In particular

   a. the relative magnitudes of intra- to interband transitions are correct.

   b. the calculations correctly predict the unexpected but observed dominance of "β"→"γ" over "β"→"g" transitions.

   c. the absolute values for the calculated "β"→"γ" and "β"→"g" matrix elements appear to be within a factor of about 2 of the data (see Section III for a more rigorous extraction of this comparison).

d. Discrepancies do appear for certain individual "γ"→"g" transitions that amount to factors of 2-4. This point has been emphasized by Bohr and Mottelson (1982) as a major discrepancy and will be discussed extensively in the next section and in Section V. For the present, it is important only to note that the discrepancies for "γ"→"g" (and "β"→"γ") transitions that do exist exhibit a systematic spin dependence that suggests a simple origin in neglected interactions.

3. The observed differences (≈20%) in the intraband rotational spacings (moments of inertia) are not reproduced and seem to be outside the scope of the simple Hamiltonian of Eq. 5, although one presumes they could be reproduced, without altering the agreement for transition rates, by the addition of higher order terms.

4. The calculations predict a K=4 band near the 0^+_3 band while experimentally the lowest K=4 band lies 300-400 keV higher. This point has been emphasized by Bohr and Mottelson (1982), who interpret the two IBA bands as double γ vibrations but argue that the high empirical energy of the K=4 band implies that the γ mode of intrinsic excitation is highly anharmonic. Therefore, they conclude that a) the low lying empirical 0^+_3 band, observed at 1422 keV, cannot be a double γ vibration, and b) that it therefore cannot correspond to the calculated band, despite the (apparently fortuitous in this view) agreement in energy. This critique undoubtedly has some merit and it would be an oversimplification to assign the empirical 0^+_3 band a purely collective character. However, the following points are also relevant. First, as will be evident in Section IV, the calculated IBA 0^+_3 excitation does not only have a large γγ' amplitude but also a strong ββ' character and admixtures of other collective modes as well. In the same vein, the 0^+_3→"γ" band transitions in the IBA calculations do not have the structure expected for γγ'→γ' transitions and, indeed (again, see Section IV), that amplitude is only one of several comparable coherent contributions to the overall 0^+_3→"γ" transition strengths. Finally, the presence of a collective $K^\pi=3^+$ band at 1656 keV suggests that it might be necessary to incorporate a g boson into the IBA description of the higher bands. (Indeed, work along this line is actively in progress (Wu, 1982; and Lin, 1982).) This additional mode is expected to have a strong effect on the K=4 band and, pending a fuller treatment of these effects, it seems premature to conclude very much about K=0 bands below 1.5 MeV from the properties of K=4 bands above 2 MeV. Nevertheless, it would not be at all surprising or unanticipated if some of the discrepancies between the predicted and observed characteristics of the 0^+_3 band could be ascribed to the presence of substantial two quasi-particle amplitudes, outside the collective IBA basis.

C. Other Deformed Nuclei

IBA calculations, as extensive as those for ^{168}Er, have not been carried out for other deformed nuclei, primarily because of the lack of the requisite detailed empirical level schemes. Even were such information available, this would not be the proper forum for such a review. Nevertheless, it is worthwhile including a few brief comments on two of the most critical characteristics of the IBA in deformed nuclei, namely the dominance of "β"→"γ" over "β"→"g"transitions and the weakness of "β"→"g" transitions compared to "γ"→"g" ones.

Concerning the first, there is very little data. These transitions are extremely weak, even if the matrix elements are large, due to the E^5_γ factor. Moreover, their transition energies are close to those of intraband transitions and thus

must be sought in complex, high background regions of the spectrum. For the most part they have only been systematically sought in (n,γ) studies utilizing the bent crystal spectrometers at the Institute Laue-Langevin in Grenoble, France for their detection. Thus far, such transitions have been observed in ^{168}Er (Davidson and co-workers, 1981), ^{158}Gd (Greenwood and co-workers, 1978), and ^{166}Er (McGowan, 1981). In each of these, a low lying K=0 band is found which predominantly deexcites to the "γ" band. In ^{156}Gd where a study (Backlin and co-workers, 1982) has also been completed, the "β" and "γ" bands are nearly degenerate and thus there is no hope of testing the prediction here. Other studies, including ones on ^{162,164}Dy, are in progress. To date, one can summarize by stating that dominant $K=0^+ \rightarrow$ "γ" transitions have been found in those cases where the empirical level spacings should permit their observations and where the appropriate studies have been carried out.

As for the second characteristic prediction, it has been well known for years that "β"→"g" transitions are empirically much weaker than "γ"→"g" transitions. Some of the data were summarized in Fig. 8. Although the relative strengths of the deexcitations of these two collective modes is beyond the scope of phenomenological geometrical models, microscopic calculations (e.g., Bes, 1963; and Bes and co-workers, 1965) in a pairing plus quadrupole formalism utilizing RPA techniques have been successful in reproducing much of the systematics. As for the IBA, not only does it reproduce this general feature, both in SU(3) and in broken SU(3) calculations (see Fig. 7), but it is an unavoidable prediction in the sense that, were the data of contrary character, one could not force the IBA to reproduce it.

It is important then to try to understand the particular characteristics of the IBA excitations that lead to such predictions, especially the ways in which they differ from the familiar geometric vibrations. The remarkable aspect is that the IBA, both here and in other situations to be encountered below, contains predictions that, to reproduce in a geometric view, require an essentially microscopic approach that explicitly treats the finite number of valence particle. Very recent results by Bijker and Dieperink (1982a) bear on this point. Through the utilization of the concept of intrinsic states, they are able to reproduce the characteristic IBA transition rate predictions of the SU(3) limit, namely that $\beta' \rightarrow g'$ transitions are weaker than $\gamma' \rightarrow g'$ by a factor of about 6 and that $\beta' \rightarrow \gamma'$ transitions dominate $\beta' \rightarrow g'$ ones. However, they also show that, as $N \rightarrow \infty$, the transition strengths, and, by implication the structure of the excitations, approach those of the geometrical picture: that is, intraband transitions dominate, followed by one phonon changing $\beta' \rightarrow g'$ and $\gamma' \rightarrow g'$ transitions, followed by two phonon changing $\beta' \rightarrow \gamma'$ transitions. Thus, it now appears that the particular uniqueness of the IBA excitations resides in differences between finite and infinite dimensional geometrical constructs, and is related to those between microscopic and macroscopic geometric models.

III. THE IBA AND GEOMETRICAL MODELS IN DEFORMED NUCLEI

The results of the previous Section show that the IBA, on the whole, successfully predicts the characteristic properties of deformed nuclei. In this Section an attempt will be made to examine two of these properties, the "γ"→"g" and "β"→"γ" transitions in the context of the familiar bandmixing formalism of the geometrical model. The motivation for this is clear. For "γ"→"g" transitions, both the IBA and the empirical branching ratios deviate from the Alaga rules. Moreover, the discrepancies between theory and experiment exhibit a spin dependence that will be seen shortly to characterize a missing bandmixing interaction. For the "β"→"γ" transitions, while they are formally forbidden in the geometrical model, it is clear if β-γ mixing is incorporated, such transitions will be allowed and will proceed by effectively intraband admixed amplitudes.

The general bandmixing formalism will first be presented below, and then, following a discussion of the application of this formalism to "γ"→"g" transitions, the structure of the IBA SU(3) wave functions for β' and γ' states will be discussed and related to the bandmixing concepts. Much of the development on this Section is taken from Casten and Warner (1981) and Warner, Casten and Davidson (1981).We thank L. L. Riedinger for much useful advice and for the derivation of Eq. 12 below.

A. Bandmixing Formalism: Mikhailov Plots

The introduction of bandmixing is a well-known and well-developed technique in the geometrical model to account for deviations of E2 branching ratios from the Alaga rules. Originally, mixing of γ and ground bands or β and ground bands was introduced to account for the "γ"→"g" and "β"→"g" B(E2) values, respectively. Later, 3-bandmixing of β, γ and g bands was included to account for small remaining discrepancies in the same B(E2) values. The 3-band mixing formalism was largely developed by Lipas (1962). It is presented in Bohr and Mottelson (1975) and, more explicitly, in a paper by Riedinger, Johnson and Hamilton (1969) which includes detailed formulae and explicit examples for ^{152}Sm and ^{154}Gd.

A.1. γ-g mixing. Consider first γ-g mixing. Following Riedinger, Johnson and Hamilton (1969) and Riedinger (1981), define admixed wave functions ψ_i for g, γ, and β bands in terms of pure wave functions ϕ_i by:

$$\psi_{I_g} = \phi_{I_g} - \varepsilon_\beta f_0(I)\phi_{I_\beta} - \varepsilon_\gamma f_2(I)\phi_{I_\gamma}$$

$$\psi_{I_\beta} = \phi_{I_\beta} + \varepsilon_\beta f_0(I)\phi_{I_g} + \varepsilon_{\beta\gamma} f_2(I)\phi_{I_\gamma} \qquad (7)$$

$$\psi_{I_\gamma} = \phi_{I_\gamma} + \varepsilon_\gamma f_2(I)\phi_{I_g} - \varepsilon_{\beta\gamma} f_2(I)\phi_{I_\beta}$$

The mixing amplitudes have been separated into spin independent parts, ε_i, and the functions $f_0(I) = I(I+1)$ and $f_2 = \sqrt{2}[(I-1)(I)(I+1)(I+2)]^{1/2}$ which give the spin dependence of the mixing for ΔK=0 and ΔK=2, respectively. With these definitions, and the assumption that the quadrupole moments are the same for each band, one obtains, in first order:

$$B(E2:I_{i\gamma}\rightarrow I_{fg}) = B_0(E2)[1+Z_\gamma F_2(I_i,I_f)-Z_{\beta\gamma}F'_{\beta\gamma}(I_i,I_f)]^2 \qquad (8)$$

where the F functions depend of $f_2(I)$ and on angular momentum coupling coefficients and $B_0(E2)$ is the unperturbed value. The parameters Z_γ and $Z_{\beta\gamma}$ are proportional to ε_γ and $\varepsilon_{\beta\gamma}$, respectively.
If one neglects the normally small β-γ mixing term, it is possible to rewrite Eq. 8 more explicitly in a particularly useful form. Thus,

$$B(E2:I_{i\gamma}\rightarrow I_{fg}) = 2\langle I_i 22-2 | I_f 0\rangle^2 \times [M_1-M_2(I_f(I_f+1)-I_i(I_i+1))]^2 \qquad (9)$$

Here, M_1 and M_2 are directly related to Z_γ($Z_\gamma = -2M_2/(M_1+4M_2)$ and are defined

$$M_1 = \langle\gamma|M(E2)|g\rangle - 4M_2 \qquad M_2 = (15/8\pi)^{1/2}Q_0(eb)\varepsilon_\gamma \qquad (10)$$

Thus, except for a correction term, M_1 is the direct intrinsic $\Delta K=2$ matrix element and M_2 is proportional to the mixing amplitude ε_γ. The advantage of the form of Eq. 9 is that it can be rewritten as:

$$\frac{\sqrt{B(E2;I_i \to I_f)}}{\sqrt{2}\langle I_i 22-2 | I_f 0\rangle} = M_1 - M_2(I_f(I_f+1)-I_i(I_i+1)) \qquad (11)$$

A plot of the left side against the spin function on the right is a straight line with intercept M_1 at $I_i=I_f$ and slope M_2. From such a plot, called a Mikhailov plot (Mikhailov, 1966), therefore, one can directly extract, from empirical results, both the direct intrinsic $\Delta K=2$ matrix element and the mixing amplitude $\varepsilon_\gamma(\propto M_2)$ provided the data can be fit by a straight line. Moreover, since, in perturbation theory, $\varepsilon_\gamma \approx \langle\psi_i | H_{pert} | \psi_f\rangle/(E_i-E_f)$, one can extract the interaction matrix element as well. Instructive examples of the use of this technique are found in Riedinger, Johnson and Hamilton (1969), Bohr and Mottelson (1975), and Warner, Casten and Davidson (1981). The latter is for ^{168}Er and is also discussed below. As noted, the Mikhailov plot formalism is useful only if the data (and any calculations) can be fit by a straight line. Deviations from a straight line can arise from several sources: unequal quadrupole moments of the bands, more than 2-band mixing [except in special cases of spin independent multiband mixing (see next Section)], or 2-bandmixing which follows a different spin dependence than that given by the $f_0(I)$ and $f_2(I)$ functions. The simple structure of Eq. 11 shows that $\Delta K=2$ bandmixing has a very systematic effect on transitions rates. First, for transitions of a given spin change, the effects must increase with increasing spin. Secondly, regardless of the sign of M_2, it follows that spin increasing transitions must deviate from the Alaga rules in a direction opposite to that for spin decreasing transitions. Both of these effects were evident in the systematics of the discrepancies between the data and the IBA in the previous section, again reinforcing the implication that those deviations arise from a partially neglected bandmixing effect in the IBA.

In Fig. 11, a Mikhailov plot for the "γ"$\to$"g" transitions in ^{168}Er is presented along with the IBA calculations (results from Table 2). It is evident that both the data and the calculations fall on good straight lines (the reason for this in the case of the IBA will be discussed in the next Section). Thus the Mikhailov analysis may be employed. The essential information contained of the plot, that is, the intercept M_1 and the slope M_2, are given in Table 4 along with the desired quantities of physical interest, the direct $\Delta K=2$ transition matrix element $\langle\gamma|M(E2)|g\rangle$, and the spin independent part of the γ-g mixing matrix element h_2. The factor of three difference in the slopes in Fig. 11 leads to progressively larger discrepancies as the level spins increase, and to the observed systematics of these discrepancies pointed out earlier. It is reflected in the extracted mixing matrix element h_2. It is important to note the enormously magnified effects of these small interactions and admixtures. Since they result in effectively intraband contributions to the coherent matrix elements, the latter can now partake of the large collectivity of rotational transitions. In particular, one notes that the discrepancies for some of the "γ"$\to$"g" transitions in fact arise because of a difference of $\approx$0.4 keV in the spin independent $\Delta K=2$ matrix element (or $\approx$3 keV in the full matrix element for 2^+ states). This difference is far beyond the scope of any reasonably expected level of agreement. Nevertheless, the concept of $\Delta K=2$ mixing is an important one in deformed nuclei and its systematics is also of high significance. The interesting point is not so much that the IBA underpredicts the mixing matrix element by 0.4 keV but that, in the context of a broken SU(3) calculation, it contains such interactions at all. Recall that they are not inherent in the pure geometrical model but must be introduced ad hoc. They do arise naturally, however, in microscopic RPA calculations of deformed

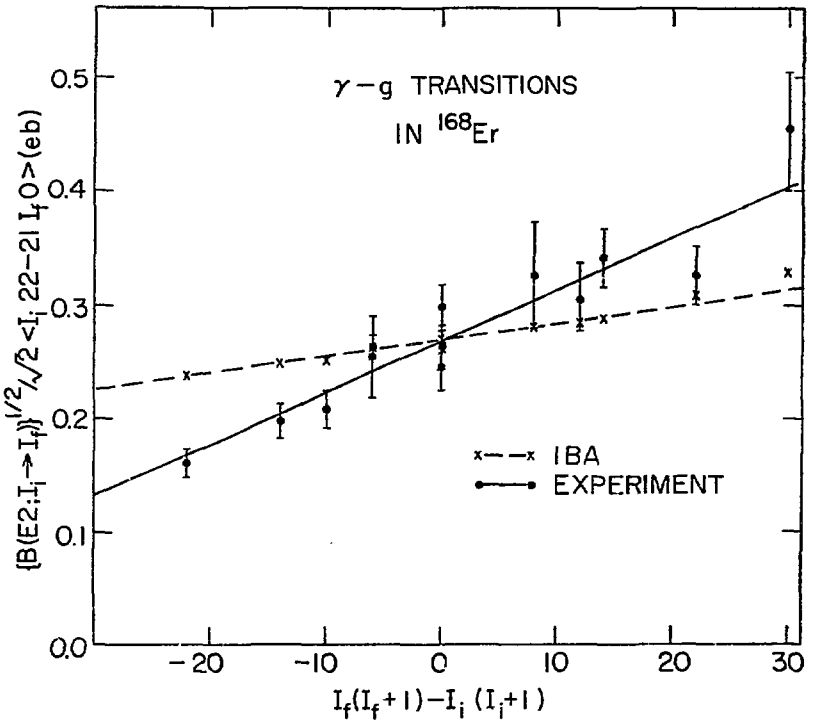

Fig. 11. Mikhailov plots (see text) for "γ"→"g" transitions in ^{168}Er (Warner, Casten and Davidson, 1981).

nuclei. Thus,again, the IBA is seen to incorporate some aspects of a microscopic treatment. (See also Section V.)

A.2. β−γ mixing. Although β−γ mixing has long been employed in the geometrical model to fine tune "γ"→"g" or "β"→"g" branching ratios, its effect on "β"→"γ"transitions themselves has not been investigated despite the fact that, by admixing an intraband amplitude, it will clearly lead to such transitions. The bandmixing formalism for "β"→"γ"transitions is similar to that for "γ"→"g"transitions since both are ΔK=2. The following expression for B(E2:γ→β) values is taken from Riedinger (1981):

$$B(E2:I_\gamma \to I_\beta) = \left\{ (2I_\gamma+1)^{-1/2} \langle \gamma \| M(E2) \| \beta \rangle + \right.$$

$$\frac{Q_{00}Q_\gamma}{Q_\beta} \left[\frac{1}{\sqrt{6}} Z_{\beta\gamma} \left[f_2(I_\beta) \langle I_\gamma 220 | I_\beta 2 \rangle - f_2(I_\gamma) \langle I_\gamma 020 | I_\beta 0 \rangle \right] \right. \qquad (12)$$

$$\left. \left. + \frac{1}{\sqrt{24}} Z_\gamma \frac{Q_\beta^2}{Q_{00}^2} f_2(I_\gamma) \langle I_\gamma 020 | I_\beta 0 \rangle + Z_\beta \frac{Q_\beta^2}{Q_{00}^2} f_0(I_\beta) \langle I_\gamma 22{-}2 | I_\beta 0 \rangle \right] \right\}^2$$

TABLE 4 Comparison of values of intrinsic and coupling matrix elements extracted from Mikhailov plots of the experimental data and the IBA predictions for ^{168}Er (from Warner, Casten and Davidson, 1981)

	Initial and final bands[a)]					
	γ → g		β → g		β → γ	
	Exp	IBA	Exp	IBA	Exp	IBA
M_1 (eb)	0.268(6)	0.269	0.039(2)	0.069	0.108(7)	0.201
M_2 (eb)	-0.0045(5)	-0.0014	-0.0006(1)	-0.0005	-0.0036(6)	0.0015
$\langle K_i \lvert M(E2) \rvert K_f \rangle$ (eb)	0.250(6)	0.263	0.039(2)	0.069	0.094(7)	0.207
$\langle K_i \lvert h_{\Delta K} \rvert K_f \rangle$ (keV)	-0.57(5)	-0.181	-0.29(5)	-0.27	0.28(5)	-0.11

a) The absolute transition strength scale was determined from the known value of $B(E2:0^+_g \rightarrow 2^+_\gamma)$ for the transitions from the 2^+_γ band, and from the predicted absolute strengths of the intraband transitions from the higher states.

where Q^2_{00}, Q^2_γ and Q^2_β are approximately proportional to the intraband, the γ→g and β→g $B(E2:0^+ \rightarrow 2^+)$ values, respectively.

Equation (12) is particularly instructive. It consists of a direct term, a first order β–γ mixing term, and two terms which arise only in a higher order mixing of the γ or β bands into the g band. The coefficient Q^2_β/Q^2_{00} is very small and so these latter terms may be neglected. The first two terms are of the same form as the first two in Eq. 8 and thus may then be cast in the form of a Mikhailov plot. However, since in the strict geometrical model the direct term is forbidden, one obtains simply

$$B(E2:I_\gamma \rightarrow I_\beta) \approx \frac{Q^2_{00} Q^2_\gamma}{6Q^2_\beta} Z^2_{\beta\gamma} G^2_{\beta\gamma}(I_\beta, I_\gamma) \qquad (13)$$

where $G_{\beta\gamma}(I_\beta, I_\gamma)$ is evident by comparison of Eqs. 12 and 13. Due to the vanishing of the direct term, this has a totally different structure than Eq. 8. There, the mixing had the effect of a correction to an existing matrix element. Since the correction term was I dependent the resultant relative B(E2) values were Z_γ dependent. Here, the $Z_{\beta\gamma}$ dependent term is not a correction but the entire source of the transition strength. Thus, whereas in Eq. 8 different values of

Z_γ altered the branching ratios, here the corresponding $Z_{\beta\gamma}$ cancels out and one has the striking result that the branching ratios are independent of $Z_{\beta\gamma}$. Therefore, while it is thus possible to obtain "β"→"γ" transitions, one cannot at all control their relative size. It is clear that the empirical average "β"→"γ"/"β"→"g" dominance can be reproduced by some choice of $Z_{\beta\gamma}$ but the spin dependence of the branching ratios will be seen below to disagree with the data, and to require for its correction the re-introduction of a direct matrix element.

First, however, one must inquire whether, indeed, the actual observed magnitude of the "β"→"γ" dominance can be reproduced by this approach for reasonable values of $Z_{\beta\gamma}$. To see this qualitatively it is sufficient, on average, to ignore the effects of β-g mixing on "β"→"g" transitions. In Eq. 13 the factor $Q^2_{00}Q^2_\gamma/6Q^2_\beta$, for typical intraband, "β"→"g" and "γ"→"g" B(E2) values in the rare earth region, is $15e^2b^2$. For moderate spins $G_{\beta\gamma}(I_\beta,I_\gamma)$ is ≈20 and so $B(E2:I_\beta\to I_\gamma) \approx (3\times10^2e^2b^2)Z^2_{\beta\gamma}$. Since typical β→g B(E2) values are on the order of 0.005 e^2b^2 the ratio $B(E2:I_\beta\to I_\gamma)/B(E2:I_\beta\to I_g)\approx(6\times10^4)Z^2_{\beta\gamma}$. To produce a ratio of 10, which is approximately the empirical value for ^{168}Er, therefore, requires a $Z_{\beta\gamma}$ of 0.013. Remarkably, this is precisely the order of magnitude of $Z_{\beta\gamma}$ values previously extracted in typical rare earth nuclei (see Riedinger, Johnson and Hamilton (1969)). Thus, one concludes that a magnitude of β-γ mixing fully consistent with previous analyses of "β"→"g" and "γ"→"g" transitions indeed leads to "β"→"γ" dominance. Before proceeding to the specific comparison of this bandmixing approach with ^{168}Er, we first consider the structure and origin of β'→γ' transitions in the IBA in relation to the above bandmixing picture.

B. Origin of β→γ Transitions in the IBA

First consider the pure SU(3) limit interpretation of β'→γ' transitions in the IBA in terms of bandmixing. Despite the apparent existence (see Fig. 5) of K=0 and K=2 bands in the (λ-4,2) representation, the structure of the IBA wave functions in the SU(3) limit is such that the "K=2" band contains a small admixture of the K=0 band (Arima and Iachello, 1978a). This is related to the fact that the wave functions of the SU(3) band can be expressed in terms of the Vergados basis whereas a scheme involving pure K bands is the Elliott basis. If $|(\lambda,\mu)\psi_2 I\rangle$ represents the SU(3) wave function in a Vergados basis for states of spin I in the band starting with I=2 in the (λ-4,2) representation, one can express this wave function in terms of the familiar Elliott basis states of good K by

$$|(\lambda,\mu)\psi_2 I\rangle = X_0|(\lambda,\mu),K=0,I\rangle + X_2|(\lambda,\mu),K=2,I\rangle$$

Clearly X_2, the coefficient of the K=2 part of this state, is ≈1. Arima and Iachello (1978a) give the following expression for X_0:

$$X_0 = -\sqrt{\frac{(I-1)(I)(I+1)(I+2)}{4(\lambda+2)(\lambda+3)(\lambda-I+2)(\lambda+I+3)}} \qquad (14)$$

which shows that X_0 is small as expected. The ratio $-X_0/X_2$ is the overlap of the K=0 and K=2 bands and is given by:

$$\langle K=0|K=2\rangle_I = \sqrt{\frac{(I-1)(I)(I+1)(I+2)}{\phi((\lambda+1,I)\phi(\lambda+2,I)}} \qquad (15)$$

TABLE 5 Overlap Amplitudes $\langle K=0 | K=2 \rangle$ of the K=0(β) in the K=2(γ) Band of the $(\lambda-4,2)$ Representation

					a) Relative Values	
	N=8	N=12	N=16	N→∞	N=16	$f_2(I)$
I=2	0.012	0.005	0.003	0	1	1
I=4	0.047	0.019	0.010	0	3.96	3.87
I=6	0.108	0.042	0.023	0	8.65	8.37
I=8	0.204	0.076	0.040	0	15.27	14.49

a) The entries for N=16 are presented again on the right, normalized to 1 for comparison with $f_2(I)=\sqrt{2}((I-1)(I(I+1)(I+2))^{1/2}$.

where $\phi(\lambda,I) = 2(\lambda+1)^2-I(I+1)$. From the structure of Eqs. 14 and 15 it is apparent that both X_0 and the overlap amplitude vanish as N(or λ)→∞.

Table 5 tabulates the overlaps for several N values and also gives the relative values for N=16 in comparison with the function $f_2(I)$ from which it is clear that this mixing in the IBA has essentially the same spin dependence as the geometric model and, again, suggests the utility of a Mikhailov analysis. With the decomposition of the SU(3) states in terms of states of good K, it is possible to write the expression for β'→γ' band E2 transitions (Scholten, 1981).

$$\langle \beta' I_\beta || M(E2) || \gamma' I_\gamma \rangle = \frac{(2I_\gamma+1)}{\sqrt{8}} \left\{ C(0,I_\beta) \left[\frac{X_0}{C(0,I_\gamma)} \begin{pmatrix} I_\gamma & 2 & I_\gamma \\ 0 & 0 & 0 \end{pmatrix} g(\lambda,I_\beta,I_\gamma) \right.\right.$$

$$+ \frac{X_2}{C(2,I_\gamma)} \begin{pmatrix} I_\gamma & 2 & I_\beta \\ 2 & -2 & 0 \end{pmatrix} \sqrt{12} \Big] + C(2,I_\beta)\langle K=0 | K=2 \rangle_{I_\beta} \left[\frac{X_0}{C(0,I_\gamma)} \begin{pmatrix} I_\gamma & 2 & I_\beta \\ 0 & 2 & -2 \end{pmatrix} \sqrt{12} \right.$$

$$\left.\left. + \frac{X_2}{C(2,I_\gamma)} \begin{pmatrix} I_\gamma & 2 & I_\beta \\ 2 & 0 & -2 \end{pmatrix} g(\lambda,I_\beta,I_\gamma) \right] \right\} \qquad (16)$$

where the C(K,I) coefficients are tabulated in Arima and Iachello (1978a) and $g(\lambda,I_\beta,I_\gamma) = 2\lambda+5+\{I_\beta(I_\beta+1)-I_\gamma(I_\gamma+1)\}/2$.

It is instructive to inspect the limiting value of Eq. 16 for large N. To do this, one needs the results that, as N→∞, the C coefficients go to zero as $\sqrt{1/\lambda}$, that the ratio of any two approaches a constant and, in particular, that $C(0,I_\beta)/C(2,I_\gamma) = 2\sqrt{(2I_\beta+1)/(2I_\gamma+1)}$. Also, $\langle K=0 | K=2 \rangle / C(2,I_\gamma)$ goes to zero as $1/\lambda^{2/3}$. Finally, from Eqs. 14 and 15, the product of either X_0 or $\langle K=0 | K=2 \rangle$ with $g(\lambda,I_\beta,I_\gamma)$ goes to zero as $1/\lambda$. Thus, Eq. 16 becomes (leaving out numerical constants)

$$\langle \beta' I_\beta \| M(E2) \| \gamma' I_\gamma \rangle \xrightarrow{N\to\infty} (2I_\beta+1)^{1/2}(2I_\gamma+1)^{1/2} \begin{pmatrix} I_\gamma & 2 & I_\beta \\ 2 & -2 & 0 \end{pmatrix}$$

$$\to (2I_\beta+1)^{1/2}\langle I_\beta 022 | I_\gamma 2\rangle \qquad (17)$$

Three important conclusions appear from Eqs. 16 and 17. First, there are two mechanisms for $\beta' \to \gamma'$ transitions: one is a direct $\Delta K=2$ intrinsic matrix element and the other stems from the K impurity of the γ' band even in the SU(3) limit. The latter mechanism vanishes in the $N\to\infty$ limit and is related to bandmixing effects in the geometrical model. The former has no analogue in the strict interpretation of that model. Second, in the infinite dimensional limit (geometrical limit), the $B(E2:\beta' \to \gamma')$ value approaches the square of a Clebsch-Gordon coefficient and therefore the IBA predicts branching ratios that approach the Alaga rules. Third, the deviations from these Alaga rules, which in the geometrical model arise from bandmixing, here arise from two sources, the K mixing just mentioned and an explicit dependence on boson number.

The essential point in determining the relation to the geometrical model is to assess the relative sizes of the direct $\Delta K=2$ and overlap contributions to the $M(E2:\beta' \to \gamma')$ in the SU(3) limit. Table 6 gives the results for several N values for the transition $2_{\beta'} \to 2_{\gamma'}$. It is clear that the direct $\Delta K=2$ term dominates, even for modest boson number. This is typical for most spins except $\Delta I=2$ transitions between high spin states where the Clebsch-Gordon coefficient for the direct term is rather small. Thus, transitions between the β' and γ' bands in the IBA in the SU(3) limit proceed predominantly by a direct $\Delta K=2$ mechanism and only to a much lesser extent via a mixing mechanism (see Warner, Casten and Davidson, 1981; and Casten and Warner (1981)).

For realistic nuclei, the SU(3) symmetry must be broken, Nevertheless, these same qualitative results persist and it will be seen, from a Mikhailov plot, that the direct $\Delta K=2$ term still dominates although its interpretation as a pure $\beta' \to \gamma'$ amplitude is altered.

TABLE 6 Magnitudes of the overlap and direct $\Delta K=2$ amplitudes in the reduced E2 matrix element for the $2^+_{\beta'} \to 2^+_{\gamma'}$ transition in the $(\lambda-4,2)$ representation

	$(\lambda-4)=12$	20	28	1000
Overlap term $K=0 \to K=0$	0.145	0.0926	0.068	0.002
Direct term $K=0 \to K=2$	2.875	2.892	2.901	2.927

C. Bandmixing Analysis of $\beta \to \gamma$ Transitions in ^{168}Er

The data and IBA calculations for "β"$\to$"γ" transitions in ^{168}Er, of course, provide an apt illustration and test of these ideas. Indeed if the data lie on a straight line in a Mikhailov plot one can extract, empirically, the relative sizes of the direct and mixing contributions to these transitions and thereby explicitly test

whether the geometrical model (with no direct matrix element) or the IBA (with dominant direct matrix element) is the more appropriate description. Figure 12 presents such a plot. The data clearly lie on a straight line (χ^2=0.5) and so does the IBA. The bandmixing points are calculated with the full Eq. 12 but with no direct term. Since only the term in Eq. 13 is significant these points closely approximate a straight line. The height of this line ($\propto Z^2_{\beta\gamma}$) was adjusted to give an overall average "β"→"γ" over "β"→"g" dominance in agreement with the data. The slope is then predetermined since, with no direct matrix element, the intercept must be $-4M_2$. While the average "β"→"γ" strength is by definition thus reproduced, the branching ratios disagree with the data. The reason is clear and significant, namely the data give explicit and direct empirical evidence for a non-zero direct ΔK=2 β→γ matrix element since the intercept of the empirical best fit line is far greater than 4 times the slope. Thus, the bandmixing approach is in disagreement with the data unless one re-introduces an ad hoc direct matrix element. Then, of course, a straight line of any desired slope may be obtained.

From the empirical and IBA lines in Fig. 12 the quantities M_1 and M_2 (and thus $\langle\gamma|M(E2)|\beta\rangle$, $\varepsilon_{\beta\gamma}$ and hence $h_{\beta\gamma}$) may be extracted. The results are included in Table 4. It is interesting to note that the magnitude of the deduced direct matrix element is between a third and half of the collective $\langle\gamma|M(E2)|g\rangle$ matrix element and thus, as with the IBA matrix element, corresponds to a definite collective enhancement. The IBA calculations, perhaps despite initial appearances in Fig. 12, are actually in rather good agreement with the data. From the Mikhailov plot for the IBA, one can deduce the size of the direct matrix element, as 0.207 eb. This is within about a factor of ≈2 of the data and is remarkable in view of the simple prescriptions used in the calculation. Finally, the slope of the IBA calculation, which appears to be in gross disagreement with the data, in fact amounts to a discrepancy of only 0.4 keV in effective spin independent interaction strength.

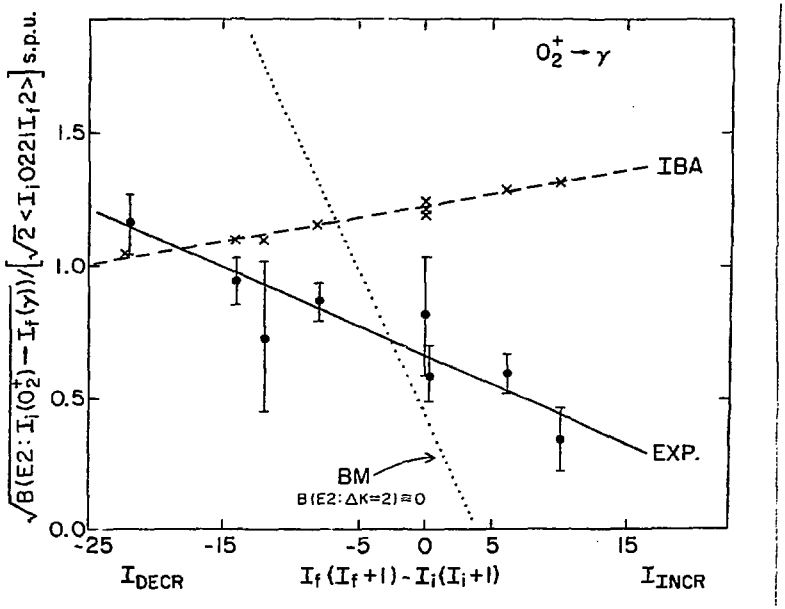

Fig. 12. Mikhailov plots (see text) for "β"→"γ" transitions in ^{168}Er (Casten and Warner, 1981).

Another point is worth mentioning. Detailed inspection (see next Section) of the IBA wave functions in these broken SU(3) calculations shows that they actually consist of amplitudes from a number of different bands and representations. Thus, it might be thought surprising that the calculated B(E2) values still yield the straight lines of Fig. 12. However, in the bandmixing formalism, the specific form of the Mikhailov plot equation (Eq. 11) arises from the assumption of the specific spin dependence of the mixing amplitudes given by the functions $f_0(I)$ or $f_2(I)$. If, however, the amplitudes are spin independent, then the relative interband B(E2) values are unaffected and a horizontal line results on a Mikhailov plot. Hence, for example, although the "β" band in ^{168}Er is composed of the β' band highly mixed with other K=0 excitations, it indeed turns out that that mixing is nearly spin independent and it is therefore not unreasonable that the IBA B(E2:"β"→"γ") values yield a straight line with slope related to the 2-band mixing of a "composite" K=0 band with a "composite" "γ" band.

For "β"→"g" transitions one can also develop a bandmixing formalism, this time incorporating ΔK=0, β→g mixing. Table 4 also includes the essential results of a Mikhailov analysis for this case for ^{168}Er. Here, the slope of the IBA predictions is almost identical with the data and very small while the predicted intrinsic matrix element is about twice the empirical value. Thus the ratio of predicted matrix elements $\langle\beta|M(E2)|g\rangle/\langle\beta|M(E2)|\gamma\rangle$ is nearly the same in the IBA and the data. Finally, the extremely small slope M_2 reflects (again see next Section) not so much negligible mixing, but rather "composite" "β" and "g" bands where the mixing is extensive but nearly spin independent.

IV. SIMPLE INTERPRETATION OF THE IBA IN DEFORMED NUCLEI

The purpose of this section is twofold, first, to analyze the form of the Hamiltonian of Eq. 5 in order to exhibit some simple properties of the resultant predictions, including a set of rather general curves which give the essential predictions by inspection in terms of a single empirical parameter, and secondly, to expand the IBA wave functions in a different basis that transparently illuminates their basic structure and the nature of the interactions that break the SU(3) symmetry. Much of the content of this section is based on Casten and Warner (1982).

A. Reduction of the Hamiltonian

The IBA Hamiltonian of Eq. 5 is suitable as a starting point for the treatment of deformed nuclei with $E"_\beta" > E"_\gamma"$. However, it is possible to substantially simplify it without losing any essential physical content. This reduction of the Hamiltonian is summarized in Table 7 along with the physical quantities calculable with it. First, one notes that the L·L term is a diagonal interaction. It cannot alter wave functions nor energy differences of states of the same spin. Next, the strengths of the Q·Q and P·P terms can be rewritten by factoring out κ. Since ε does not appear in this Hamiltonian, the SU(5) basis states that are admixed by H (see Table 1) are degenerate and the combination of Q·Q and P·P represents a particular set of SU(5) symmetry breaking matrix elements. Thus the resultant mixing must be independent of the overall scale factor, κ. This coefficient, however, will clearly affect the final energy scale. Therefore, as long as one considers only wave functions, transition rates and the ratios of energies for states of the same spin, or alternately these energy differences to within a scale factor, the final Hamiltonian in Table 7 gives the same results as the initial one. But the reduced Hamiltonian has only a single parameter $\kappa"/\kappa$. This has the value 0 for SU(3) and in the limit $(\kappa"/\kappa)\to\infty$, the O(6) limit is obtained. Thus, for a given N,

all results of an IBA calculation in this framework for deformed nuclei can be specified in terms of this parameter (and χ for E2 transition rates), and therefore plotted as general curves from which one may read off the relevant predictions. It will be seen shortly that this parameter can in fact be empirically specified and thus the Hamiltonian reduction is not merely a mathematical simplification but provides a practical tool as well.

TABLE 7 Reduction of the IBA Hamiltonian for Deformed Nuclei

Hamiltonian	Calculable Physical Quantities
$H = -\kappa\, Q\cdot Q - \kappa' L\cdot L + \kappa'' P\cdot P$	E,ψ, trans. rates (B(E2))[a]
Delete $\downarrow$ $\kappa' L\cdot L$	
$H = -\kappa\, Q\cdot Q + \kappa'' P\cdot P$ $= -\kappa\, [Q\cdot Q - (\kappa''/\kappa)\, P\cdot P]$	$E_i(I)-E_j(I),\psi,$ trans. rates (B(E2))[a]
Ignore $\downarrow$ κ	
$H \approx Q\cdot Q - \kappa''/\kappa\, P\cdot P$	$(E_i(I)-E_j(I))/\kappa,\psi,$ trans. rates (B(E2))[a]

a) B(E2) values require the further specification of χ in T(E2). However, to good approximation for initial or schematic calculations this can be fixed at a global value of -0.85 corresponding to the mean value of the narrow acceptable range for deformed nuclei.

The results for 2^+ energy levels, for N=16, are shown in Fig. 13. (Note that the symmetry breaking parameter in Fig. 13, and in similar figures below, is given as $\kappa''/4\kappa$ since this quantity is identical to the ratio, -"PAIR"/"QQ", of the two corresponding input quantities to the IBA-1 code PHINT.)

The behavior of these energy levels is noteworthy. First, the 2^+"$_\gamma$" level is hardly affected by the P•P interaction, thus justifying, retroactively, the use of the SU(3) expressions (Eq. 4) to fix κ and κ' in carrying out a broken SU(3) IBA calculation. Secondly, the first excited $K=0^+$ band rises rapidly in energy. So do the second and third 0^+ bands. The behavior of the "β" band (0^+_2) in fact suggests a way of empirically defining the symmetry breaking. Note that the quantity $E_{2^+\text{"}\beta\text{"}}/E_{2^+\text{"}\gamma\text{"}}$ is a unique function of $\kappa''/4\kappa$ and thus can be used to specify the latter. But, since this in turn specifies the entire calculated set of predictions corresponding to the reduced Hamiltonian, those predictions can be directly inferred from the empirical parameter itself. In practice, it turns out that the 0^+"$_\beta$" level is more commonly known and therefore a better choice of parameter is $E_{0^+\text{"}\beta\text{"}}/(E_{2^+\text{"}\gamma\text{"}}-E_{2^+\text{"}g\text{"}})$. Furthermore, since $\kappa''/4\kappa \to 0$ in the SU(3) limit, it is convenient to have the empirical substitute parameter do the same and, therefore, it is best to adapt $[(E_{0^+\text{"}\beta\text{"}}/(E_{2^+\text{"}\gamma\text{"}}-E_{2^+\text{"}g\text{"}}))-1]$. This

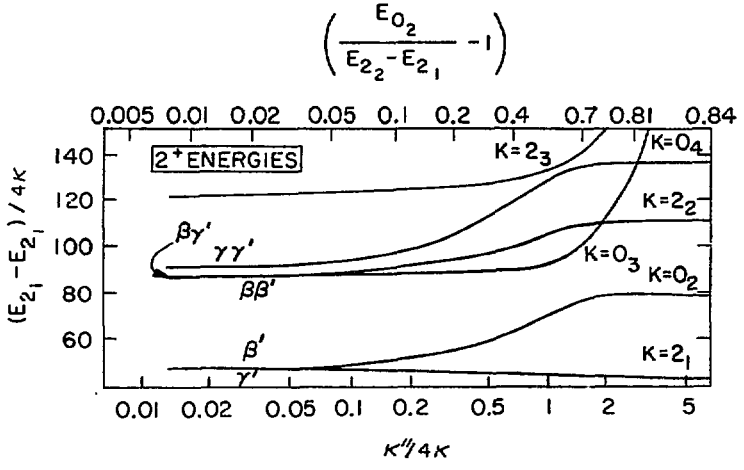

Fig. 13. Relative 2^+ energies as a function of SU(3) symmetry breaking for N=16. The levels are labelled by the SU(3) description on the left and by the dominant K quantum numbers on the right. The subscripts refer to the ordinal number of the band of that K. Note that the 2^+ level of the ground band is not shown and thus there is a suppressed zero on the ordinate side (Casten and Warner, 1982).

alternate scale is given across the top in Fig. 13 and, in subsequent figures below, may be substituted freely for the $\kappa''/4\kappa$ scale. Note that, since the "β" band energy eventually flattens out for large symmetry breaking this parameter approaches a constant value. At that point (roughly for $\kappa''/4\kappa > 2$) its utility decreases rapidly. However, for most empirical nuclei, E''_β/E''_γ ranges from 1.0-1.7 so that the usable range coincides with the important range.

B. Transformation to SU(3) Basis

As illustrated in Table I, the IBA wave functions for deformed nuclei are extremely complex in the SU(5) basis. Transition rates, which involve two states, are even more complex. For example, for N=16 there are 51 2^+ states in IBA-1. In deformed nuclei there will be large amplitudes for a considerable fraction of these SU(5) basis states. A B(E2) value will involve a linear contribution of over 2500 products of these amplitudes each involving a relevant elementary SU(5) E2 matrix element: many of these will vanish but a large number will have comparable contributions. Moreover, each such contribution corresponds to a transition in a vibrational nucleus with no easy interpretation in a deformed context.

However, if the wave functions are re-expanded in SU(3) one might reasonably expect a substantial simplification. This has been studied in Casten and Warner (1982). In practice such a transformation is made trivial ly using the existing

IBA program PHINT (Scholten, 1977) to give both the actual wave functions and those of SU(3). To illustrate these ideas, the expansions of the low lying 2^+ states are given in Figs. 14 and 15, for N=16. [They were obtained with the code IBAOVL written to calculate such overlaps (and also B(E2) expansions). It is available on request.] The behavior is extremely simple. Each state is pure in SU(3) but of course becomes admixed as the symmetry breaking is introduced. For orientation, most typical deformed nuclei correspond to $\kappa''/4\kappa$ values between 0.4 and 1. (In ^{168}Er, $\kappa''/4\kappa = 0.94$). In no case are more than four or five amplitudes required to effectively describe the low lying states.

Although the results shown in Figs. 14 and 15 are for 2^+ states, similar conclusions apply for other spins so we shall henceforth refer to the structure of the various "bands". The "g" and "γ" bands are particularly simple, each being for the most part an admixture of one other band. The "β" band, initially situated between the g' and $\beta\beta'$ bands mixes substantially with both. The 0^+_3 band, initially $\beta\beta'$, mixes so strongly with the close lying $\gamma\gamma'$ band that the two soon interchange character.

The most striking feature of Figs. 14 and 15 is that, for each state, the strongly admixed amplitudes always have the same K value (with one exception discussed below). Thus, the SU(3) symmetry breaking corresponds simply to $\Delta K=0$ interactions between certain pairs of bands. The simplicity and elegance of this result is manifest. One can go further, however, and extract the size of the $\Delta K=0$ matrix elements. In Casten and Warner (1982) this was done in a crude but simple way for the $\beta\beta'$-$\gamma\gamma'$ mixing by noting that, for $\kappa''/4\kappa < 0.5$, one could approximate the 0^+_3 wave function by a 2-state admixture. Then it is trivial to work backwards from

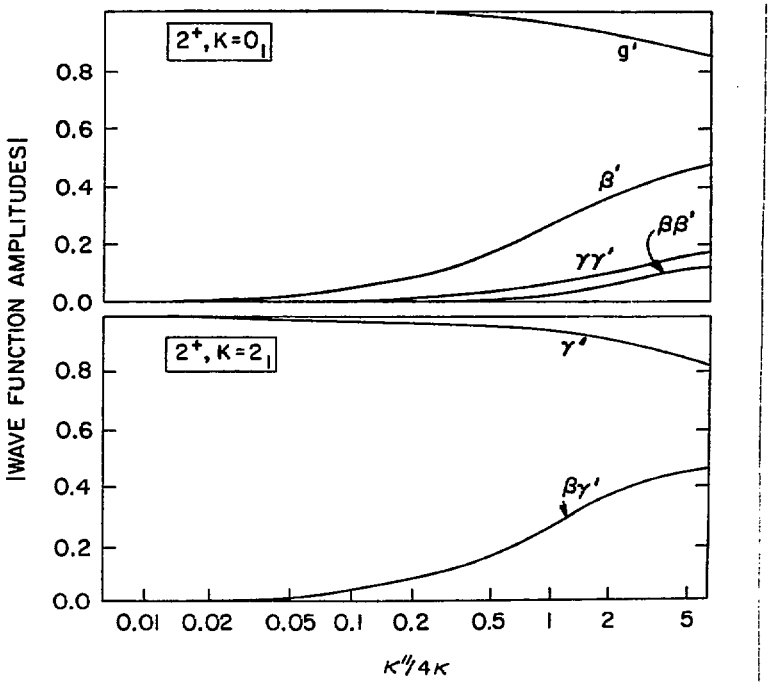

Fig. 14 Major amplitudes in the expansion of the 2^+"g" and 2^+"γ" states in SU(3) for N=16.

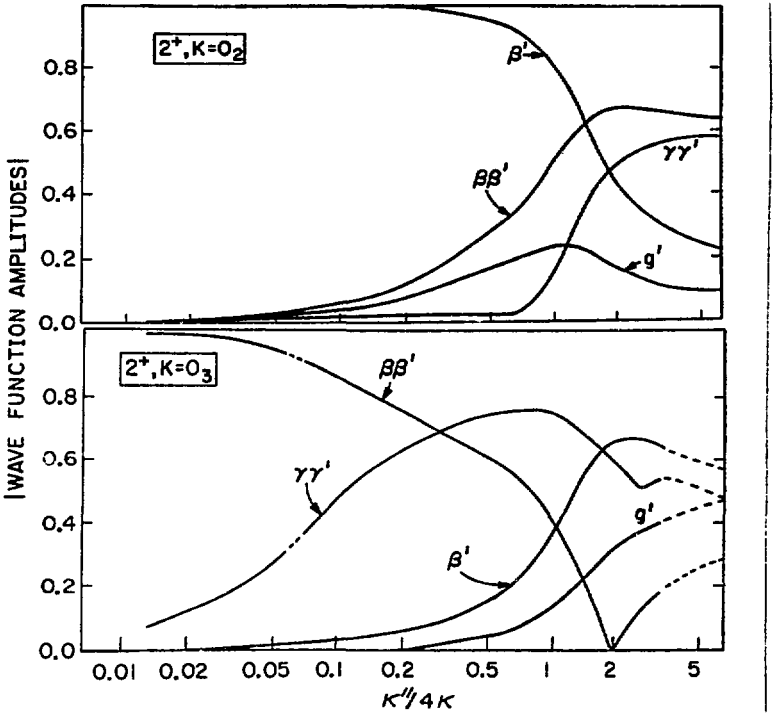

Fig. 15. Major amplitudes in the expansion of the 2"β" and the 2^+ state of the 0^+_3 band in SU(3) for N=16 (Casten and Warner, 1982).

the final energies and admixtures to obtain, as a function of $\kappa''/4\kappa$, the implied $\Delta K=0$ matrix elements between the SU(3) states. Note that, over a narrow region near $\kappa''/4\kappa \approx 0.06$ in Fig. 15, the ββ' and γγ' amplitudes are dashed. This was done since over that region there suddenly occurs very large $\Delta K=2$ mixing between the ββ' and βγ' amplitudes. This arises because these two states are initially degenerate in SU(3) but move slightly apart from diagonal contributions from the P·P interaction while, at the same time, there is a matrix element between them which, though remaining very small, grows with symmetry breaking. Over this particular narrow region, its ratio to the unperturbed energy separation is large. This fortuitous occurence allows the extraction, in a similar 2-state approximation, of a $\Delta K=2$ matrix element as well. It was found to be ≈ two orders of magnitude weaker than the $\Delta K=0$ matrix element.

Of course, the more rigorous way to extract the matrix elements between SU(3) states is by directly transforming the initial Hamiltonian into the SU(3) basis. In matrix notation, where U is a matrix of SU(3) wave functions in the SU(5) basis and where $H_v(5)$ is the perturbation matrix also in SU(5) basis, then the interaction matrix $H_v(3)$ expressed in the SU(3) basis is given by:

$$H_v(3) = U^T H_v(5) U$$

where U^T is the transpose of U.

Application of this transformation then gives the ΔK=0 coupling matrix elements, not only for ββ' and γγ' bands and for κ"/4κ ranges where the 2-state mixing approximation is valid, but for all bands and parameter values. Moreover, it gives the full set of small ΔK=2 matrix elements as well. It is obvious from the reduced Hamiltonian of Table 7 that the effect of κ"/4κ itself is simply a scaling of the SU(3) symmetry breaking interaction. Thus, all non-diagonal matrix elements simply scale as κ"/4κ and these matrix elements will thus preserve a constant ratio. These last two statements imply that a log-log plot of the interaction matrix elements in an SU(3) basis vs. κ"/4κ consists of a series of parallel straight lines. Their relative heights depend only on the structure of the P•P interaction expressed in the SU(3) basis. As an example, the matrix elements deduced from this transformation are illustrated, for N=16, in Fig. 16. (The values for the ββ'↔γγ' matrix element, deduced in Casten and Warner (1982) by a 2-state mixing analysis, are essentially identical with those of the figure for κ"/4κ < 1.) Note that the ΔK=0 matrix elements shown are all roughly the same size and, in each case, admix SU(3) bands from adjacent representations. Weaker ΔK=0 matrix elements between non-adjacent representations also exist but are not plotted.

Now, the simplicity of the IBA scheme is apparent. In it, deformed nuclei are characterized as composed of states represented by simple linear combinations of SU(3) states coupled by large (several 100 keV typically) ΔK=0 matrix elements and very small (<10 keV) ΔK=2 matrix elements.

A note regarding the relation to bandmixing is relevant here. In the geometrical model, the bandmixing formalism allows one to account for tiny mixtures among g, β and γ bands. But these elementary excitations themselves are, in effect, pre-adjusted phenomenologically for each nucleus, and cannot be directly compared across large regions. In the IBA the elementary modes are the SU(3) states which, aside from a small N dependence, are the same throughout a deformed region. They

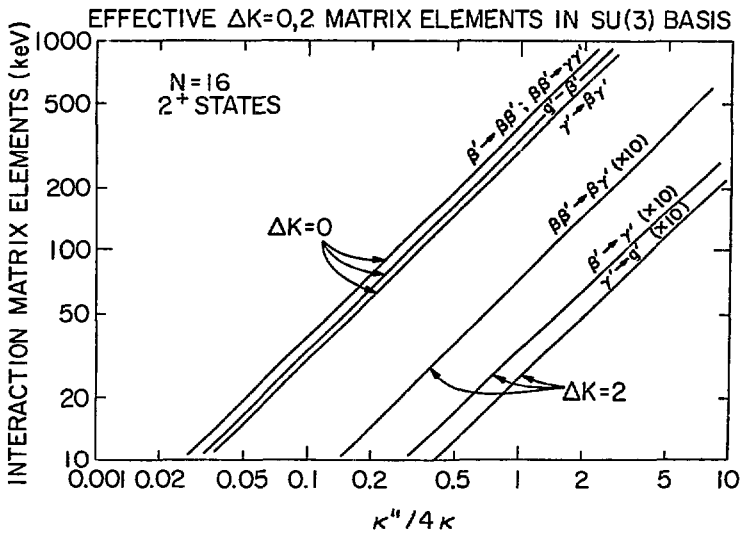

Fig. 16. Principal ΔK=0 and ΔK=2 matrix elements between low lying SU(3) states as a function of the SU(3) symmetry breaking for N=16.

are admixed by relatively large ΔK=0 matrix elements. The uniformity of the basis yields some qualitative a priori predictions. For example, the large ΔK=0 matrix element, its sensitivity to $\kappa''/4\kappa$, and the fact that there are many more low lying K=0 than K=2 excitations leads to the general expectation that the "γ" band will be relatively constant in structure across a deformed region whereas the "β" band will show much greater variability. It is evident from Fig. 8 that this accords with the experimental facts.

C. Composition of Transition Rates

It is tempting to exploit the simplicity of the IBA wave functions in the SU(3) basis to decompose the calculated transition rates. With the use of this expansion any B(E2) value can be written as a linear combination of terms, each of which contains the product of a pair of SU(3) amplitudes in the initial and final wave functions, and the elementary E2 matrix element between those two SU(3) states. The elementary SU(3) E2 matrix elements must, of course, be calculated with the same value of χ as in the actual IBA calculation.

Since each wave function contains only 2-4 major SU(3) amplitudes and since some SU(3) E2 transition rates are identically zero for any χ value (if $\Delta(\lambda,\mu)>4$) there will typically be only ≈2-6 significant contributions to each B(E2) value. Since the wave functions are known as a function of $\kappa''/4\kappa$, the composition of any E2 matrix element can be similarly plotted. Figure 17 shows two examples for deexcitation of the "β" band, and Fig. 18 shows, in bar graph form, the specific amplitudes for four transitions in ^{168}Er.

In both examples in Fig. 17, and indeed for any transition, the M(E2) in the SU(3) limit consists of only a single amplitude corresponding to the transition between the SU(3) states involved. As the $\kappa''/4\kappa$ (i.e., P·P) symmetry breaking is introduced, the newly emerging amplitudes in the initial and final wave functions introduce other coherent contributions. In many cases for $\kappa''/4\kappa$ values typical of deformed nuclei (roughly 0.3-1.5), amplitudes other than the original one can be rather substantial or can even dominate.

For transitions between states which are primarily mutual admixtures of two SU(3) states, the coherent sum contains two "diagonal" terms, that is, terms proportional to the SU(3) state quadrupole moments. Orthonormality requires that these amplitudes will have opposite sign. Then, under the usual situation with quadrupole moments of the same sign, these two contributions to the E2 matrix element will tend to cancel. Moreover, since the quadrupole moments are of intraband magnitude, any differences in them can lead to incomplete cancellation which can easily dominate the net transition strength even for a rather small degree of symmetry breaking. This happens, for example, in the "β"→"g" transition. The relevant quadrupole moments will differ most, leading to the strongest "β"→"g" transitions (for a given degree of symmetry breaking), for small boson number, that is, near the edges of the deformed region. In the geometric model, a qualitative microscopic analysis (Bohr and Mottelson, 1975), in terms of the E2 selection rules in the Nilsson scheme, ascribes a similar origin to the "β"→"g" transitions in terms of differing quadrupole moments of specific Nilsson orbits. Once again, it appears that there is a correspondence between the IBA and microscopic collective models.

The other transitions in Figs. 17 and 18 are also of interest. The "β"→"γ" transition clearly mirrors the results obtained earlier from a bandmixing analysis of the ^{168}Er calculations, namely that the dominant mechanism is the direct ΔK=2, β'→γ' matrix element. The relative purity of the "γ"→"g" transition is evident in

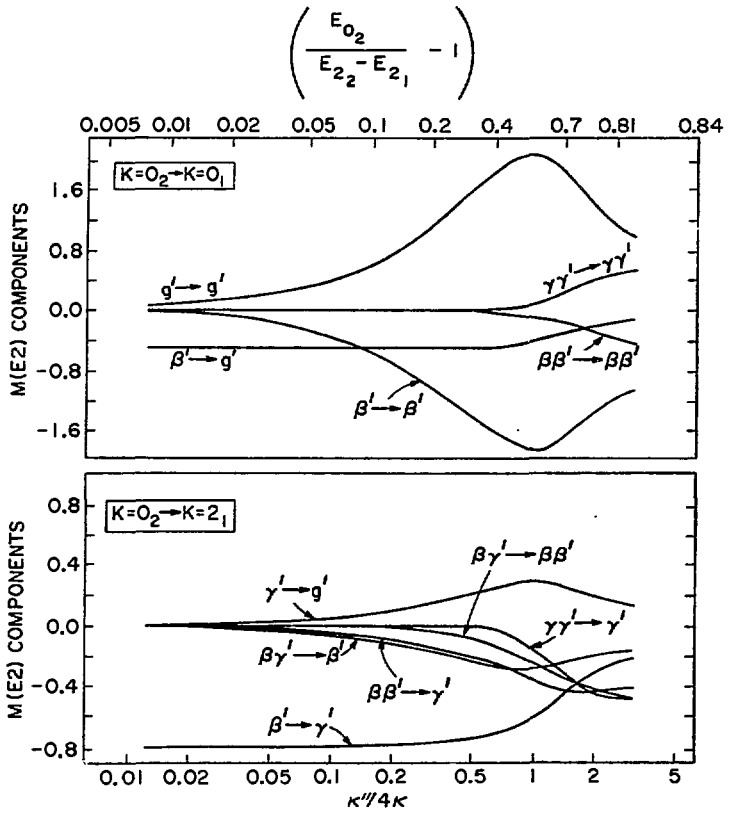

Fig. 17. Principal SU(3) contributions for two B(E2) values as a function of SU(3) symmetry breaking for N=16 (Casten and Warner, 1982).

Fig. 18 and, again, is a reflection of the statement made earlier that the γ band, which admixes strongly primarily only with the βγ' band, will remain relatively pure and stable across a deformed region.

Finally, the 0^+_3→"γ" transition, from the second excited 0^+ band in ^{168}Er, is seen in Fig. 18 to be rather complex. The γγ'→γ' amplitude is indeed the largest, and the net coherent amplitude happens to approximate this contribution but the actual calculated transition is composed of several comparable amplitudes. The final transition strength depends at least as much on the detailed coherence of these other amplitudes as it does on the γγ'→γ' amplitude. Moreover, as discussed in Section II, the γγ' SU(3) state itself is not simply a double γ' mode. Thus, the relationship of the IBA "γγ" K=0 excitation to the analagous geometrical state, and in particular, its labelling as a γγ phonon state, is by no means obvious.

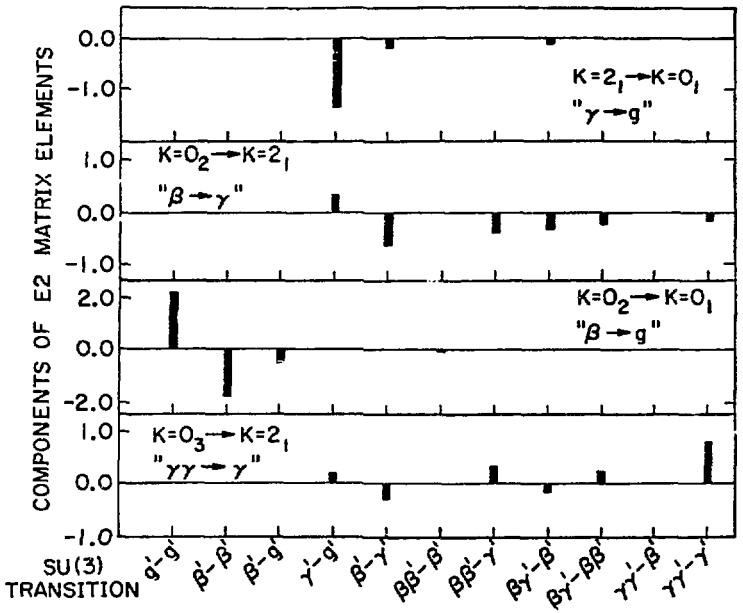

Fig. 18. Composition, in bar graph form, for four E2 transitions for the specific value of $\kappa''/4\kappa$ (0.94) appropriate to ^{168}Er (Casten and Warner, 1982).

V. REVISED FORMULATION OF THE IBA

A. Motivation and Formulation for a Modified Hamiltonian

Despite the success of the IBA for deformed nuclei, there is one disquieting element in the formalism. It will be recalled from the discussion of Section II that the coefficient χ in the E2 operator has been determined empirically to have a value near -0.85 in deformed nuclei whereas the analogous coefficient χ_Q in the Q operator of the Hamiltonian is fixed at $\chi_Q = -2.958$. If the quadrupole operator has a physical significance as such, it would clearly be preferable to utilize the same form in both instances.

The effects of such a modification have recently been studied (Warner and Casten, 1982a). As noted in conjunction with the earlier discussion of Table I, the P•P term has Δn_d=0 and 2 terms while Q•Q has Δn_d=0,1 and 2 terms. If the coefficient χ_Q in Q is reduced, reference to Eq. 2 shows that one of the effects will be to reduce the size of the Δn_d=1 term in Q•Q relative to the Δn_d=2 term: but this is exactly the primary effect of the P•P term. So one might hope that utilizing the same value of χ_Q in the Hamiltonian and E2 operator would avoid the need for a P•P term in H, or at least, limit the role of a smaller P•P term to a fine tuning mechanism.

Thus, one is motivated to propose (Warner and Casten, 1982a) the following Hamiltonian

$$H' = \varepsilon n_d - \kappa Q' \cdot Q' - \kappa' L \cdot L \qquad (18)$$

where Q' is more defined as in Eq. 2 but χ_Q now takes on the same value as χ in T(E2). (Henceforth, we refer to these now equal coefficients as χ_Q.) The expected range of χ_Q as before lies between 0 and -2.958.

B. Reduction of the Hamiltonian

This is an extremely simple Hamiltonian and it remains to be shown if it is adequate. First, however, it is worthwhile analyzing it along the lines of Section IV.A (see Table 7). First, for deformed nuclei with $E"_\beta" > E"_\gamma"$ one may omit the εn_d term. Secondly the L•L term is diagonal, and thus cannot affect energy differences of states of the same spin. As before, wave functions and transition rates are unaffected by the scale factor κ. Thus the calculation of all wave functions, transition rates and relative energy differences of the form $(E_i(I) - E_j(I))/\kappa$, depends only on the single parameter χ_Q. By choosing some B(E2) ratio that is insensitive to changes in the wave functions such as the ratio used earlier to determine χ, namely $B(E2:2^+_\gamma \rightarrow 0^+_g)/B(E2:2^+_g \rightarrow 0^+_g)$, χ_Q may be fixed from an empirical branching ratio.

C. Comparison with Earlier Results

One is almost reluctant to expect that such a simplified approach could work but the motivation for modifying the Q operator in H seems so compelling that it is worth testing how the new formalism works. To do this, the extensive and detailed results for ^{168}Er provide a stringent test where the original formalism was rather successful. To carry out such a test, the χ_Q value for this nucleus was determined according to the procedure above and a value of -1.1 was obtained. Whereas, previously, the wave functions could be calculated once and for all for a given value of $\kappa"/4\kappa$ and then χ varied, now each χ_Q value in T(E2) represents in effect a different Hamiltonian and hence a different eigenvector equation. Thus it is natural that the new χ_Q value differs somewhat from the earlier value of -0.68. It might be recalled that the earlier value of χ for ^{168}Er was but one example of a narrow range of χ values valid for the whole rare earth region. When the present formalism is applied over this same region, a similarly narrow range is again obtained, namely $-1.5 \leq \chi_Q \leq -0.9$.

With the new value of $\chi_Q = -1.1$ for ^{168}Er the level energies and E2 transition rates may be calculated. The results are compared with those obtained (Warner, Casten and Davidson, 1980 and 1981) earlier in Fig. 19. (Of course, to normalize the absolute energy scale in the χ_Q formalism part of the figure, a specific value for κ was used.) The results are striking. First, without a P•P term, the present formalism reproduces almost exactly the same energy level sequence, band for band. (For simplicity, only bandheads are shown in the figure since rotational spacings are essentially unchanged.) Secondly, the principal calculated B(E2) values are almost unchanged. Specifically, the ratio of interband to intraband strengths (exemplified by the "γ"→"g" strengths, since the intraband strengths are normalized to each other) is identical. Secondly, the "β"→"γ" transitions again dominate the "β"→"g". The first noticeable difference occurs in the "β"→"g" transitions which are weaker in the new formalism. But this is in better agreement with experiment since in Tables 2 and 3, and the discussion surrounding them, it was pointed out that the "β"→"g" transitions were overpredicted by a factor of ≈4. The largest change noted in Fig. 19 is in the 0^+_3→"β" transitions but here no comment relative to experiment can be made since no such transitions

were observed. Thus, as far as can be determined, the present formalism, with one parameter less, is at least as much in accord with the data as the earlier one. Indeed, it is actually in better agreement in some respects. This is most apparent if the "γ"→"g" transitions are considered in detail, analogous to the earlier discussion of Table 2. However, instead of repeating such a table one may take advantage of the bandmixing/Mikhailov formalism. Given that a set of data and calculations lie on straight lines on a Mikhailov plot, the extraction of the direct matrix element and the Z coefficient from such a plot is fully equivalent to the detailed presentation of the complete table and may be substituted for it. (As an aside, it is worth noting the power and simplicity of this oft-neglected formalism.)

Figure 20 repeats the Mikhailov plots of Fig. 11 and adds the line corresponding to the "γ"→"g" matrix elements of the new formalism. One may argue the significance of the earlier factor of three difference in slope between the IBA and the data, and hence of comparable differences in a few B(E2) values between the higher spin states, arising as they did from the magnified effects of very small interactions. Nevertheless, it is striking that the new formalism, again with one less parameter, now correctly reproduces even the fine details of the ΔK=2 mixing.

The origin of the improvement is still being studied, but the following two points may be mentioned. In general, comparable fits to the level energies in the two

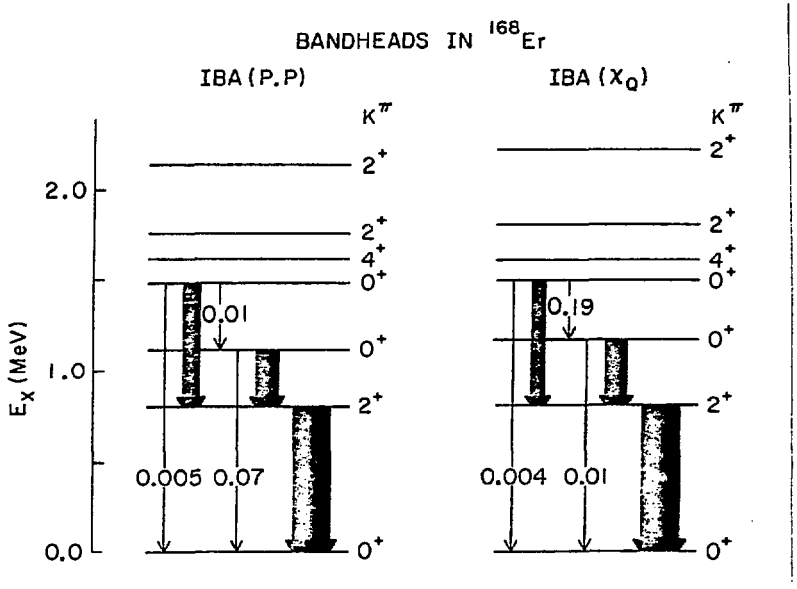

Fig. 19. Comparison of calculated level energies of ^{168}Er (bandheads only, rotational spacings are similar in the two calculations) in the original IBA-1 formalism for deformed nuclei in which the SU(3) symmetry is broken with a P·P interaction and in the modified formalism incorporating a variable X_Q in the Hamiltonian (Warner and Casten, 1982a).

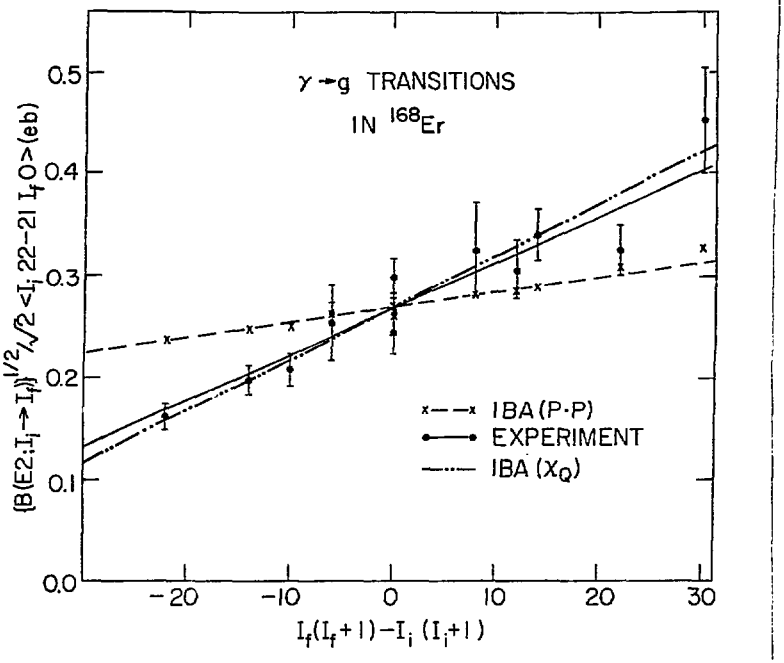

Fig. 20. Mikhailov plot for "γ"→"g" transitions in ^{168}Er. Same as Fig. 11 but showing also the calculated results of the new (χ_Q) formalism (Warner and Casten, 1982a).

formalisms result in wave functions that, overall, are very similar in structure. Both approaches result in the breaking of SU(3) by strong $\Delta K=0$ and much weaker $\Delta K=2$ interactions. However, in both, the symmetry breaking has two effects, one a diagonal contribution to the SU(3) energies, and the other due to off-diagonal mixing matrix elements. Comparable final energies emerge from the new formalism by a different combination of the two contributions, specifically, smaller diagonal energy shifts and larger mixing matrix elements, both $\Delta K=0$ and $\Delta K=2$. Thus, the wave functions in the modified formalism are rather more mixed. For transitions, such as "γ"→"g" and "β"→"γ", which arise primarily (see Figs. 17 and 18) from the dominant SU(3) amplitudes of the parent pure states, the greater admixtures of small amplitudes has little effect and thus similar B(E2) predictions result. For transitions, such as "β"→"g" which arise primarily from cancellations, stemming from coherent contributions involving relatively small wave function amplitudes, the altered mixing in the present formalism is significant. Finally, since the $\Delta K=2$ matrix elements are also larger in this formalism, the γ'→g' mixing is larger and the Mikhailov plot for the IBA exhibits a larger slope.

One may inquire if this improved agreement for the "γ"→"g" transitions is an isolated case. To test this, similar calculations have been performed for an extensive series of deformed rare earth nuclei. For each, χ_Q was fixed from the usual B(E2) ratio. This then fixed all other B(E2) values and comparison tables can be constructed. Again, though, the entire content of a series of such tables

is contained, as far as deviations of the interband B(E2) values from the Alaga rules is concerned, from a plot of the calculated and empirical Z_γ factors. The results of this comparison of Z_γ values is presented in Fig. 21, along with some early microscopic values calculated in a RPA scheme by Bes and co-workers (1965). Remarkably, the IBA predictions of this extremely sensitive (see earlier discussion) quantity are in excellent agreement with the data over an extensive set of nuclei. Nowhere is there more than a factor of 2 discrepancy. Moreover, both the data and the calculations exhibit the same characteristic systematics, which are quite regular, especially when plotted against boson number instead of nucleus, showing a parabolic behavior, minimizing at mid-shell. This behavior is not surprising in the context of familiar rotation-vibration coupling ideas. Near the edges of the deformed region the separation of these two degrees of freedom is imperfect and thus they mix much more extensively than in the center of the deformed region. The origin of the systematics in the IBA calculations is twofold. First, there is a variation in Z_γ as a function of χ_Q which is separately fitted for each nucleus. Secondly, however, the $\Delta K=2$ matrix elements, and hence the Z_γ values, exhibit a sharply decreasing behavior with increasing boson number, N. Since χ_Q falls in a relatively narrow range, it is not surprising that the boson number effects represent a significant contribution to the parabolic systematics just noted.

D. The O(6) Limit: A Special Case

If the new formalism is to be regarded as a substitute for the earlier one it should not lose any of the characteristic features formerly present. In

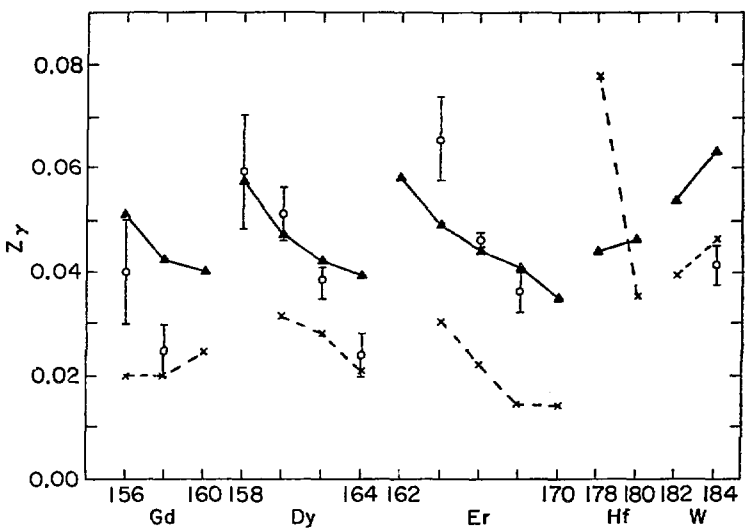

Fig. 21. Systematics of empirical values (points) of Z_γ extracted for rare earth nuclei with E"β" > E"γ" in comparison with the IBA predictions (solid lines) in the modified formalism and with microscopic calculations of Bes and co-workers (1965) (dashed line). (From Warner and Casten, 1982a.)

particular each of the characteristic limits should be recovered. Clearly the SU(5) limit can be obtained from Eq. 18 when ϵ is large just as in the earlier case. More worrisome at first is the O(6) limit (Arima and Iachello, 1978b). Its characteristic term (see Eq. 1) was the P•P term which is now absent. Moreover, the actual O(6) spectrum arises in the earlier formalism, Eq. 1, only by inclusion of three independent terms, namely

$$H = -\kappa L\cdot L + \kappa'' P\cdot P + T_3(d^+\tilde{d}^+)^{(3)}(\tilde{d}\tilde{d})^{(3)} \tag{19}$$

In the new formalism this limit must correspond to $\chi_Q=0$ which makes Q' a generator of O(6). Then H' becomes

$$\begin{aligned} H' &= -\kappa Q'\cdot Q' - \kappa' L\cdot L \\ &= -\kappa(s^+\tilde{d}+d^+s)^{(2)}\cdot(s^+\tilde{d}+d^+s)^{(2)} - \kappa' L\cdot L \end{aligned} \tag{20}$$

which contains only two independent terms.

Thus, while the O(6) wave functions result for $\chi_Q=0$, the eigenvalue expression clearly cannot be identical since H in Eq. 19 gives rise to an eigenvalue equation with three coefficients,

$$E(\sigma,\tau,L) = (A/4)\ (N-\sigma)\ (N+\sigma+4) + B\tau(\tau+3) + CL(L+1) \tag{21}$$

whereas for H' the resulting eigenvalue expression can contain at most 2 parameters and is given by

$$E'(\sigma,\tau,L) = A'[(N-\sigma)\ (N+\sigma+4) + \tau(\tau+3)] + C'L(L+1) \tag{22}$$

Thus, an O(6) limit is obtained, but it is a special case of the earlier one corresponding to A/4=B. This, per se, is not a difficulty and there is no inherent reason that empirical nuclei should exhibit this related parameter dependence. Recall that, analogously, SU(3) is a special case of deformed nuclei with $E(2^+)_{\beta'} = E(2^+)_{\gamma'}$. Nevertheless, since the O(6) limit is so well manifested in the Pt region, especially ^{196}Pt, it is interesting to compare Eq. 22 with the values for A and B extracted earlier (Cizewski and co-workers, 1978) for ^{196}Pt. The latter were A=185 keV, B=43 keV. Remarkably, these are almost exactly in the ratio 4:1 in striking support of a new formalism incorporating a variable χ_Q in the Hamiltonian.

E. Contour Plots and Parameter-free Predictions of Energy and B(E2) Ratios

The fact that both SU(3) and O(6) schemes are contained in the new formalism leads to some interesting parameter-free predictions of qualitative systematics. A range of nuclei spanning these two limits corresponds to a range of χ_Q from -2.958 to 0. Any energy or B(E2) ratio can now be calculated as a function of χ_Q for different N values and a contour plot against N and χ_Q constructed. Examples are given in Figs. 22 and 23. For any given nucleus of interest, of course, χ_Q can be determined and the appropriate quantity read off the plots. [Note: It is strongly emphasized that these or similar plots are not to be taken as the IBA predictions: they are only the results of the extremely simplified truncation of the Hamiltonian and should be considered as a starting point for actual calculations. Despite the apparent success of this simple approach, it is anticipated that many specific calculations will require the re-introduction of a P•P term, albeit almost certainly of smaller magnitude.] However, the principal

purpose of such plots is not this, but to illustrate that they provide qualitative parameter-free predictions of the generalized trajectories or systematics across a transition region. Thus, for example, since the O(6) limit has $\chi_Q=0$ and, typically, N≈6, while deformed nuclei have $\chi_Q \approx -0.9$ to -1.5 and N≈12-16, a B(E2) ratio in an O(6) to SU(3) transition will follow a path from roughly the lower left corner to the upper center.

Consider the ratio $B(E2:2^+_\gamma \rightarrow 0^+_g)/B(E2:2^+_g \rightarrow 0^+_g)$. In O(6), this is zero (the transition in the numerator is forbidden) and it is also very small in SU(3) (ratio of inter- to intraband transitions). From Fig. 22, however, it is clear that the IBA predicts, unambiguously, and independent of the details of parameter fitting, that this branching ratio must peak in the intermediate transition region, and at a value of the order of ≈0.1 or less. In general these qualitative trends are reflected empirically in the Pt-W nuclei in further support of the IBA.

Figure 23 shows similar plots of the "β" band (Warner, Casten and Dejbakhsh, 1982). It is clear that, within the realm of deformed nuclei ($-1.5 \leq \chi_Q \leq -0.9$), the $B(E2:2^+_\beta \rightarrow 0^+_g)$ is approximately 50-200 times weaker than the $B(E2:2^+_\gamma \rightarrow 0^+_g)$ value. The energy contour plot shows that this band will lie between ≈1.4-1.7 times the γ band energy. Both these predictions are qualitatively in accord with a large body of data. Since there is no parameter in the new formalism that is fitted with any reference to the "β" band, these results imply that the predicted "β" band properties are coupled to those of the "γ" band whose properties are used to fit χ_Q. Thus the qualitative agreement just noted is a rather stringent test, and the implied relation between these collective modes an intriguing concept.

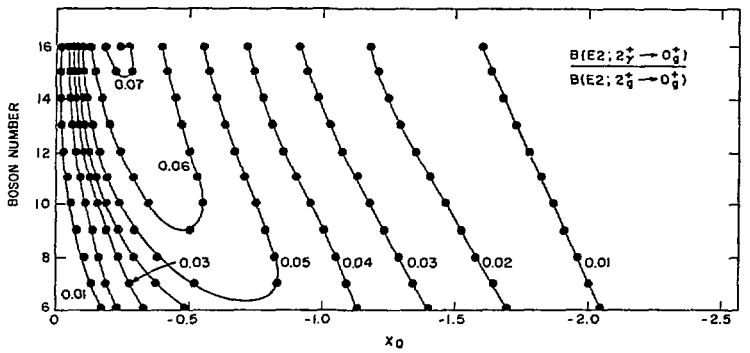

Fig. 22. Contour plot of a B(E2) ratio in the modified formalism. Typical O(6) and SU(3) nuclei correspond to the extreme lower left and the upper center, respectively (Warner and Casten, 1982a).

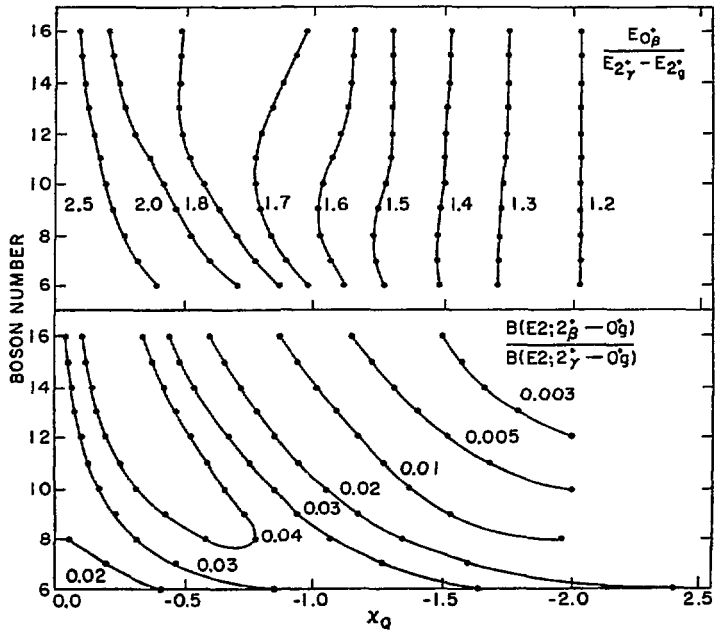

Fig. 23. Contour plot of energy and B(E2) ratios relating the "β" and "γ" bands (Warner, Casten and Dejbakhsh, 1982).

F. Relation to IBA-2

The IBA-2, which distinguishes proton and neutron bosons, is clearly more ammenable to a microscopic derivation of its parameters and thus is linked to shell model concepts of generalized seniority and pair occupation. Since it has been noted that the IBA-1 contains many features relating to finite particle number, it would be tremendously advantageous to relate it to the IBA-2. The IBA-2 Hamiltonian (Otsuka and co-workers, 1978; Otsuka, Arima and Iachello, 1978; Iachello, 1979; Scholten, 1979; Bijker and co-workers, 1980; Duval and Barrett, 1981a), as conventionally used (i.e., somewhat truncated from the complete one) is

$$H_2 = \varepsilon(n_{d_\pi} + n_{d_\nu}) - \kappa Q_\pi \cdot Q_\nu + \text{diagonal terms in } (d^+d^+)^{(L)}_{\pi(\nu)}(\tilde{d}\tilde{d})^{L}_{\pi(\nu)} \qquad (23)$$

where Q is defined as in Eq. 2 for either protons or neutrons. The precise relationship between the IBA-1 Hamiltonian of Eq. 1 and this IBA-2 Hamiltonian is hardly immediately transparent although projection formulae connecting the two have been suggested (Scholten, 1980). In the Hamiltonian of the new formalism, given in Eq. 18, however, the form of the quadrupole operator is now the same as in Eq. 23 and there is a closer analogy to the IBA-2 Hamiltonian.

There is already one recent (Bijker and Dieperink, 1982b) result which emphasizes this connection. These authors have, for the first time, worked out the symmetry structure of the IBA-2, in terms of group chains based on U(6)xU(6) and obtain each of the three characteristic IBA-1 limits (plus, incidentally, a fourth corresponding to triaxial nuclei). However, the O(6) limit turns out to be a special case of the general O(6) limit of IBA-1. Remarkably, it is exactly the same special case, with A/4=B, as obtained for the O(6) limit in the present revised formulation of the IBA-1.

VI. SUMMARY

There are too many individual points to offer a complete summary. Rather, we may schematically review the foregoing by emphasizing a few of them.

The structure and characteristic properties and predictions of the IBA in deformed nuclei have been reviewed, and compared with experiment, in particular for ^{168}Er. Overall, excellent agreement, with a minimum of free parameters (in effect, two, neglecting scale factors on energy differences), was obtained.

A particularly surprising, and unavoidable, prediction is that of strong "β"→"γ" transitions, a feature characterically absent in the geometrical model, but manifest empirically. Some discrepancies were also noted, principally for the K=4 excitation, and the detailed magnitudes of some specific B(E2) values. Considerable attention was paid to analyzing the structure of the IBA states and their relation to geometric models. The bandmixing formalism was studied to interpret both the aforementioned discrepancies and the origin of the "β"→"γ" transitions.

The IBA states, extremely complex in the usual SU(5) basis, were transformed to the SU(3) basis, as was the interaction Hamiltonian. The IBA wave functions appear with much simplified structure in this way, as does the structure of the associated B(E2) values. The nature of the symmetry breaking of SU(3) for actual deformed nuclei was seen to be predominantly $\Delta K=0$ mixing.

A modified, and more consistent, formalism for the IBA-1 was introduced which is simpler, has fewer free parameters (in effect, one, neglecting scale factors on energy differences), is in at least as good agreement with experiment as the earlier formalism, contains a special case of the O(6) limit which corresponds to that known empirically, and appears to have a close relationship to the IBA-2. The new formalism facilitates the construction of contour plots of various observables (e.g., energy or B(E2) ratios) as functions of N and χ_Q which allow the parameter-free discussion of qualitative trajectories or systematics.

Several general themes recur throughout. First the IBA works rather well in deformed nuclei. Secondly, its principal predictions can be obtained with a minimum of parameters and can be understood rather simply. Thirdly, the IBA contains a number of striking, characteristic, and empirically verified, predictions, such as the strong "β"→"γ" transitions, the dominance of "γ"→"g" over "β"→"g" transitions, the contribution to "β"→"g" transitions from differences in parent SU(3) state quadrupole moments, the approximately parabolic systematics in Z_γ and the predicted energy and B(E2) ratio trajectories of the revised formalism, and others, not discussed above, such as the systematics in the decay of 0^+ states in near O(6) nuclei (Casten and Cizewski, 1978; Casten, 1979). Notably, many of these arise in the IBA precisely due to the explicit inclusion of finite boson number effects. Given this, it is hardly surprising that these features can be reproduced in geometric models by the introduction of perturbations, to the simple harmonic picture, whose origin is known to be essentially microscopic. These

conclusions suggest, in turn, that the IBA-1, though evidently phenomenological in its approach, is intermediate between phenomenological and microscopic in its predictive power, due largely to the incorporation of finite boson number.

VII. ACKNOWLEDGEMENT

It is a pleasure to acknowledge with gratitude invaluable discussions with F. Iachello, A. Arima, I. Talmi, A. Dieperink, H. Feshbach, P. Brentano, A. Gelberg, O. Scholten, J. Cizewski, W. F. Davidson, B. Barrett, R. Gilmore, D. H. Feng, F. Stephens, L. Riedinger, J. Wood, K. Heyde, S. Pittel, A. Bohr and B. R. Mottelson.

Research has been performed under contract DE-AC02-76CH00016 with the U.S. Department of Energy.

REFERENCES

Arima, A. and Iachello, F. (1975). Phys. Rev. Lett., 35, 1069.

Arima, A. and Iachello, F. (1976). Ann. Phys. (N.Y.), 99, 253.

Arima, A. and Iachello, F. (1978a). Ann. Phys. (N.Y.), 111, 201.

Arima, A. and Iachello, F. (1978b). Phys. Rev. Lett., 40, 385.

Backlin, A., Hedin, G., Fogelberg, B., Savaceno, R. C., Greenwood, R. C., Reich, C. W., Koch, H. R., Baader, H. A., Breitig, H. D., Schult, O. W. B., Schreckenbach, K., von Egidy, T. and Mampe, W. (1982). To be published.

Bes, D. R. (1963). Nucl. Phys., 49, 544.

Bes, D. R., Federman, P., Maqueda, E. and Zuker, A. (1965). Nucl. Phys., 65, 1.

Bijker, R. and Dieperink, A. E. L. (1982a). Preprint and private communication.

Bijker, R. and Dieperink, A. E. L. (1982b). Preprint and Lectures, this conference.

Bijker, R., Dieperink, A. E. L., Scholten, O. and Spanhoff, R. (1980). Nucl. Phys., A344, 209.

Bohr, A. and Mottelson, B. R. (1975). In Nuclear Structure, Benjamin, New York, Vol. II.

Bohr, A. and Mottelson, B. R. (1980). Physica Scripta, 22, 468.

Bohr, A. and Mottelson, B. R. (1982). Physica Scripta, 25, 28.

Casten, R. F. (1979). In F. Iachello (Ed.), Interacting Bosons in Nuclear Physics, Plenum Press, New York. p. 37.

Casten, R. F. (1980). Workshop on Nuclear Physics, Drexel University, to be published.

Casten, R. F. (1981). In F. Iachello (Ed.), Interacting Bose-Fermi Systems in Nuclei, Plenum Press, New York. p. 3.

Casten, R. F. and Cizewski, J. (1978). Nucl. Phys., A309, 477.

Casten, R. F. and Warner, D. D. (1981). In Neutron Capture Gamma-Ray Spectroscopy and Related Topics, Inst. of Physics, Conf. Series No. 62. p. 28.

Casten, R. F. and Warner, D. D. (1982). Phys. Rev. Lett., 48, 666.

Cizewski, J. A., Casten, R. F., Smith, G. J., Stelts, M. L., Kane, W. R., Borner, H. G. and Davidson, W. F. (1978). Phys. Rev. Lett., 40, 167.

Davidson, W. F., Casten, R. F., Warner, D. D., Schreckenbach, K., Borner, H. G., Simic, J., Stojanovic, M., Bogdanovic, M., Koicki, S., Gelletly, W., Orr, G. B. and Stelts, M. L. (1981). J. Phys. G., 7, 455 and 843.

Greenwood, R. C., Reich, C. W., Baader, H. A., Koch, H. R., Breitig, D., Schult, O. W. B., Fogelberg, B., Backlin, A., Mampe, W., von Egidy, T. and Schreckenbach, K. (1978). Nucl. Phys., A304, 327.

Iachello, F. (1979). In F. Iachello (Ed.), Interacting Bosons in Nuclear Physics, Plenum Press, New York. p. 1.

Iachello, F. (1981a). In C. Abrahams, K. Allaart and A. E. L. Dieperink (Eds.), Dronten Nuclear Structure Summer School, Plenum Press, New York.

Iachello, F. (1981b). In Neutron Capture Gamma-Ray Spectroscopy and Related Topics, Inst. of Physics Conf. Series, No. 62. p. 15.

Kaup, U. and Gelberg, A. (1979). Z. Phys., A293, 311.

Lin, Y. (1982). Preprint.

Lipas, P. O. (1962). Nucl. Phys., 39, 468.

McGowan, F. K. (1981). Phys. Rev., C24, 1803.

McGowan, F. K. and Milner, W. T. (1981). Phys. Rev., C23, 1926.

Mikhailov, V. M. (1966). Izv. Ahad. Nauk. Ser. Fiz., 30, 1334 and Bull. Acad. Sci. U.S.S.R. Phys. Ser., 30, 1392.

Otsuka, T., Arima, A. and Iachello, F. (1978). Nucl. Phys., A309, 1.

Otsuka, T., Arima, A., Iachello, F. and Talmi, I. (1978). Phys. Lett., 76B, 139.

Riedinger, L. L. (1981). Private communication.

Riedinger, L. L., Johnson, N. R. and Hamilton, J. H. (1969). Phys. Rev., 179, 1214.

Sage, K. and Barrett, B. R. (1980). Phys. Rev., C22, 1765.

Sambataro, M. and Molnar, G. (1982). Nucl. Phys., A376, 201.

Scholten, O. (1977). Code PHINT, unpublished.

Scholten, O. (1979). In F. Iachello (Ed.), Interacting Bosons in Nuclear Physics, Plenum Press, New York. p. 17.

Scholten, O. (1980). Thesis.

Scholten, O. (1981). Private communication.

Stachel, J., Van Isacker, P. and Heyde, K. (1982). Phys. Rev., C25, 650.

Talmi, I. (1979). In F. Iachello (Ed.), Interacting Bosons in Nuclear Physics, Plenum Press, New York. p. 79.

Van Isacker, P., Heyde, K., Waroquier, M. and Wenes, G. (1981). Phys. Lett., 104B, 5.

Van Isacker, P., Heyde, K., Waroquier, M. and Wenes, G. (1982). Nucl. Phys., A380, 383.

Warner, D. D. (1981). Phys. Rev. Lett., 47, 1819.

Warner, D. D. and Casten, R. F. (1982a). Phys. Rev. Lett., 48, 1385.

Warner, D. D. and Casten, R. F. (1982b). Phys. Rev., C25, 2019.

Warner, D. D., Casten, R. F. and Davidson, W. F. (1980). Phys. Rev. Lett., 45, 1261.

Warner, D. D., Casten, R. F. and Davidson, W. F. (1981). Phys. Rev., C24, 1713.

Warner, D. D., Casten, R. F. and Dejbakhsh, H. (1982). Contribution to the International Conference on Nuclear Structure, Amsterdam.

Wu, H. C. (1982). Phys. Lett., 110B, 1.